Available online at www.sciencedirect.com

ScienceDirect

Ceramics International 37 (2011) 1705–1724

CERAMICS INTERNATIONAL

www.elsevier.com/locate/ceramint

Review paper

Spinel-containing alumina-based refractory castables

M.A.L. Braulio [a], M. Rigaud [b], A. Buhr [c], C. Parr [d], V.C. Pandolfelli [a,*]

[a] Federal University of São Carlos Materials Engineering Department Materials Microstructure Engineering Group km 235, Rod. Washington Luís, 13565-905, São Carlos, SP, Brazil (FIRE Associate Laboratory)
[b] École Polytechnique, Campus Université de Montréal Montréal, QC, H3C 3A7, Canada
[c] Almatis GmbH, Frankfurt Main, Germany
[d] Kerneos, Paris, France

Received 3 January 2011; received in revised form 11 January 2011; accepted 14 February 2011
Available online 8 April 2011

Abstract

Due to their high corrosion resistance to basic slags, either pre-formed or *in situ* spinel ($MgAl_2O_4$) containing refractory castables are nowadays widely used as steel ladle linings. Nevertheless, whereas the pre-formed spinel castables present high volumetric stability and a well-known processing technology, the *in situ* spinel castables still require further understanding due to the challenges related to magnesia hydration and their expansive behaviour at high temperatures. Therefore, the objective of this paper is to review the knowledge already available for high-alumina spinel-containing castables (preformed and *in situ*) in order to provide a support for novel technological developments in the area. The main variables considered are the spinel content and grain size, the effect of calcium aluminate cement and hydratable alumina on the general castables' properties, the influence of different alumina and magnesia sources and the silica fume content. Nowadays research subjects, including the use of mineralising compounds, the addition of nano-scaled particles and the evaluation of the effect of expansion under constraint will also be addressed, pointing out alternatives for the design of high-performance alumina-magnesia refractory castables.

Keywords: Refractories (E); Spinels (D)

Contents

---

1. Introduction

Magnesium aluminate spinel is a member of a class of minerals that have the same crystal structure, which is called the spinel group. The general formula of the spinel group is AB_2O_4, where A represents a divalent metal ion such as

---

* Corresponding author.
E-mail address: vicpando@power.ufscar.br (V.C. Pandolfelli).

0272-8842/$36.00 © 2011 Elsevier Ltd and Techna Group S.r.l. All rights reserved.
doi:10.1016/j.ceramint.2011.03.049

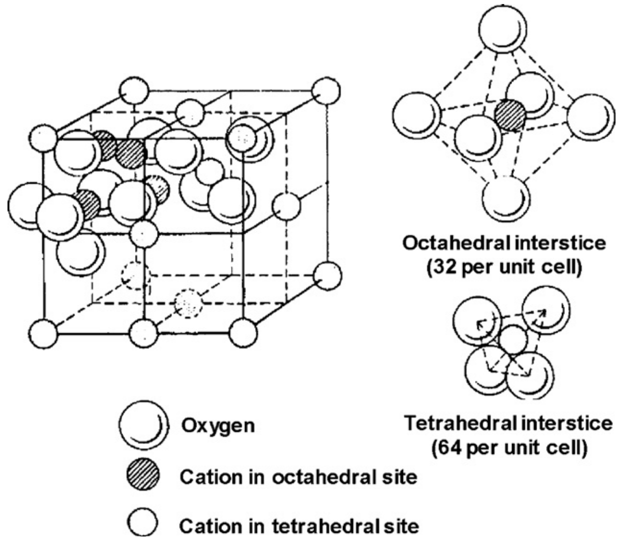

Fig. 1. Cubic crystalline structure of spinel [1].

magnesium, iron, nickel, manganese and/or zinc, and B represents trivalent metal ions such as aluminium, iron, chromium or manganese. Unless otherwise described, the term ''spinel'' in this paper will refer to $MgAl_2O_4$, which is the only compound in the binary system MgO - Al_2O_3. Stoichiometric spinel presents a molar ration of 1 MgO to 1 Al_2O_3 and comprises 71.67 wt% Al_2O_3 and 28.33 wt% MgO.

The spinel crystal structure (Fig. 1) is built by a cubic dense packing of oxygen anions, where half of the octahedral voids are occupied by aluminium cations, and only every eighth tetrahedral void is occupied by magnesium cations. Both magnesium and aluminium cations can be replaced by other metal cations of the same electrical charge, which enables a wide range of solid solutions. The anionic oxygen lattice changes only slightly if at all, so that the XRD patterns of spinel solid solutions remain very similar.

Additionally, the $MgAl_2O_4$ structure shows an increasing phase region that scales with the temperature (Fig. 2), especially towards higher alumina contents. That means $MgAl_2O_4$ can form broad solid solutions with its components, MgO and Al_2O_3. Electrochemical balance is attained by vacancies at metal-cation and oxygen-anion sites in the structure. Moreover here, the lattice dimensions remain practically unchanged. This feature will be discussed later as it plays an important role in defining the advantage of spinel for resistance to steel-making slag.

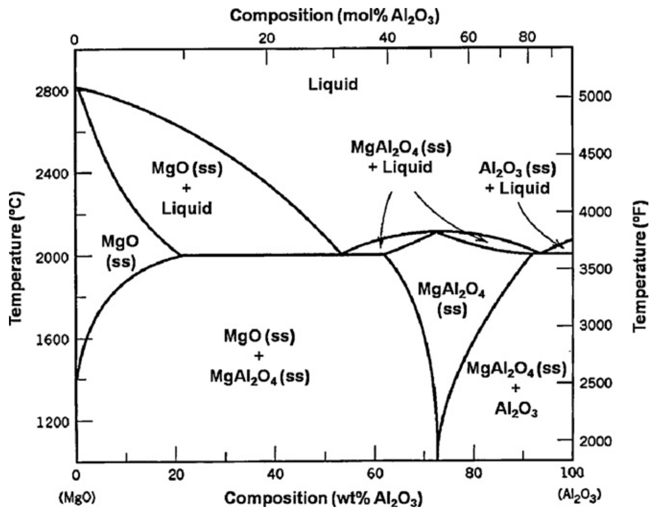

Fig. 2. Magnesia - alumina phase diagram [2].

Table 1 summarises important technical properties of spinel when compared to magnesia and corundum [1–3]. The differences between the thermal expansion of these phases are partially responsible for the superior thermal shock resistance of spinel containing refractories. The decrease in density associated with the respective increase in specific volume as spinel forms from magnesia and corundum, needs to be considered for technical applications, e.g. in castables, where spinel is formed *in situ* from MgO and Al_2O_3 components. According to Bradt [4], spinel can be considered as the ''mullite of the XXI century'' due to its high melting point temperature and chemical stability.

Natural sources of spinel as refractory raw material are not known. Therefore, it must be synthetically produced either by a sintering or a fusion process. The differences between these two process routes and the properties of different spinel raw materials are discussed by Racher et al. [5]. It is important to use high purity raw materials to produce high performance spinel raw materials. When bauxite is used instead of synthetic alumina, the resulting spinel will perform worse, e.g. thermomechanical properties as shown by Moore et al. [6].

Synthetic spinels have been used in refractories since the 1980 s, first as an addition to fired magnesia bricks for cement kilns as an alternative to magnesia-chrome bricks to overcome health concerns [7]. These spinels have either magnesia rich or stoichiometric composition. In the late 1980 s, spinel containing alumina refractories were also developed, especially castables for steel ladle lining in Japan. However, magnesia rich spinels have shown disadvantages for such applications because they are designed to contain traces of free magnesia. Therefore, new alumina rich spinel raw materials were developed [8–10] and became standard materials especially for steel ladle applications.

Table 1
Thermal and physical properties of spinel, periclase and corundum [1–3].

Properties	$MgAl_2O_4$	MgO	Al_2O_3
Melting point (°C)	2135	2852	2054
Thermal expansion ($.10^{-6}$/°C)			
100 °C	5.6	10–12	5.6
500 °C	7.6	11–13	7.3–8.0
1000 °C	8.4	13–15	8.7–9.3
1500 °C	10.2	15–19	9.3–9.9
Thermal conductivity (W/mK)			
25 °C	15	40	38
100 °C	13	38	36
500 °C	8	16	11
1000 °C	5	7	7
Density (g/cm^3)	3.58	3.65	3.99

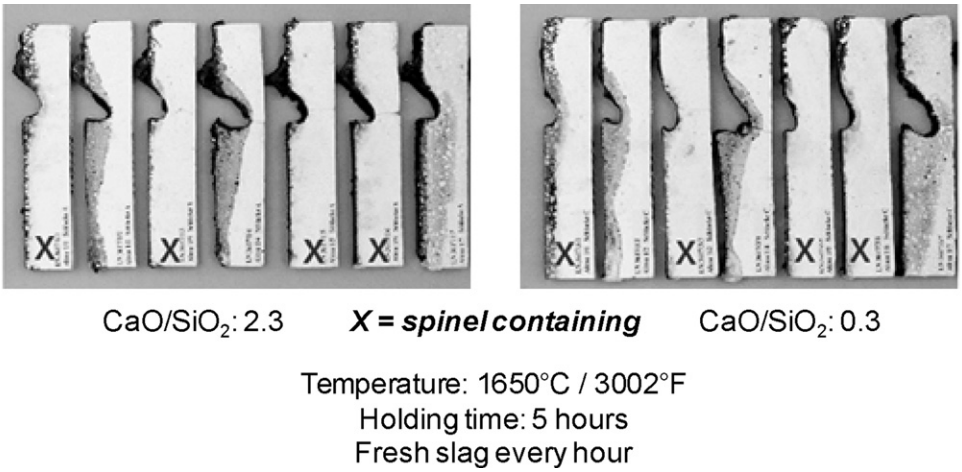

Fig. 3. Induction furnace slag corrosion test of alumina and alumina-spinel castables [5].

In the 1990 s, a second group of spinel castables was developed. Instead of pre-reacted spinel, these castables contain free magnesia in the matrix fines, which form spinel by reacting with alumina during use at high temperatures (*in situ* spinel formation) [11–17]. Spinel forming castables have shown advantages when compared to spinel containing ones in steel ladle side wall lining and have become a common material for this region in the past 20 years. For other applications, e.g. well blocks and purging plugs, spinel containing castables are advantageous and have become the standard accordingly. Both concepts show characteristic features which will be discussed in the following sections.

2. Preformed spinel-containing castables

Preformed spinel is added to alumina castables for two major purposes: to increase the slag resistance and to improve the thermo-mechanical properties. Fig. 3 shows the results of a slag corrosion test of various alumina and alumina-spinel castables in an induction furnace. The spinel containing castables show less penetration and less corrosion when compared to the pure alumina ones in both cases, basic and acidic slag composition [5].

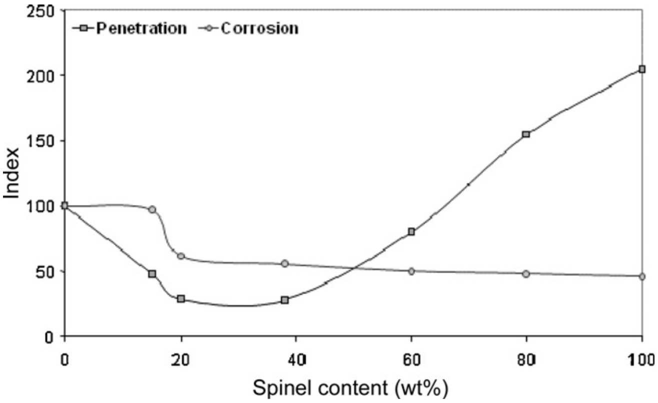

Fig. 4. Spinel content effect on the slag penetration and corrosion resistance [23].

The slag resistance and wear mechanism of spinel castables in contact with steel-making slag has been investigated by various authors [8–10,15,18–22]. The optimal spinel content is in the range of 15 to 30 wt%, preferably between 20 and 25 wt%. If too little spinel is added, it results in a higher corrosion rate whereas if there is too much spinel, it leads to high penetration (Fig. 4) because the spinel does not react with the infiltrating slag [23]. Alumina rich spinels such as AR 78 and AR 90 (numbers indicate the alumina content in wt%) provide advantages when compared to stoichiometric spinel [10,20,22,24]. FeO and MnO of the infiltrating slag can be entrapped on lattice vacancies in the alumina rich spinel solid solution and both the slag melting point temperature and viscosity increase thus inhibiting further penetration. The CaO of the slag reacts with alumina to form high melting calcium hexaluminate and calcium dialuminate.

Another important aspect is the grain size of the spinel. Spinel must be added predominantly to the fine fraction of the castable formulation to attain the best penetration resistance (Fig. 5 [25]) based on industrial experience over the past 20 years. According to Reisinger et al. [26], a spinel containing matrix improves the corrosion behaviour of a castable

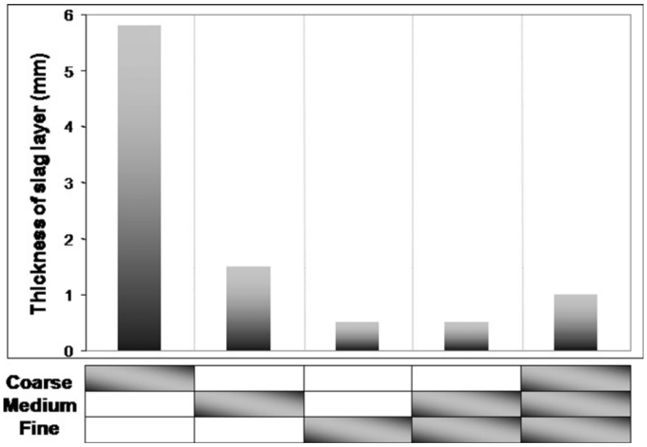

Fig. 5. Relationship between the spinel grain size (coarse, medium, or fine) and the thickness of the penetrated slag layer [25].

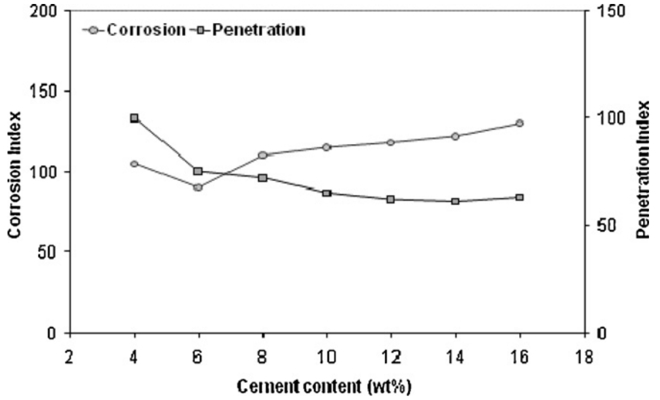

Fig. 6. Corrosion and slag penetration resistance of alumina-spinel castables containing different cement contents [27].

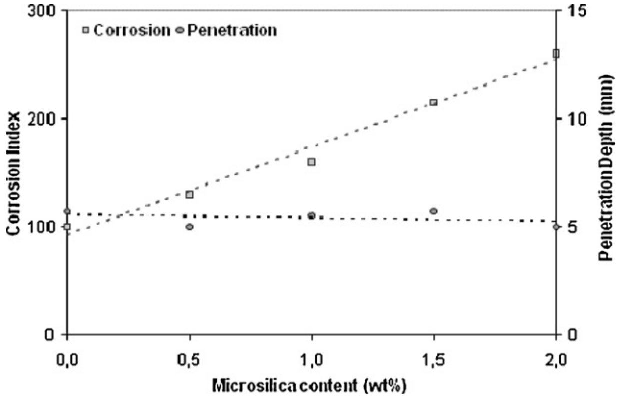

Fig. 8. Effect of silica fume addition on the slag resistance (corrosion and penetration) of alumina-spinel castables [24].

independently, whether the spinel has been added as such to the matrix, whether it developed due to the reaction of alumina with added fine magnesia, or it is formed "*in situ*" together with the MgO of the infiltrating slag. Two important aspects for improved corrosion resistance are the total amount of spinel and its distribution with respect to particle size. Yamamura et al. [27] investigated corrosion and penetration resistance of alumina-spinel castables with different cement content (Fig. 6) and found an increasing corrosion with higher cement contents but decreasing penetration. Today most of the alumina-spinel castables are low cement castables (1 - 2.5 wt% CaO).

The thermo-mechanical properties such as hot modulus of rupture (HMoR) and refractoriness under load (RuL) of alumina castables are considerably improved by adding high purity spinel as shown by various authors [5,27,28]. For instance, Kriechbaum et al. [29] observed an increase of HMoR at 1500 °C from 8 to 17 MPa when spinel fines were added to a tabular alumina based low cement castable. Ko [24,30] found an increase of HMoR from 1300 to 1500 °C and associated it with the bridging between the alumina rich spinel grains and the calcium hexaluminate crystals formed at high temperatures (Fig. 7).

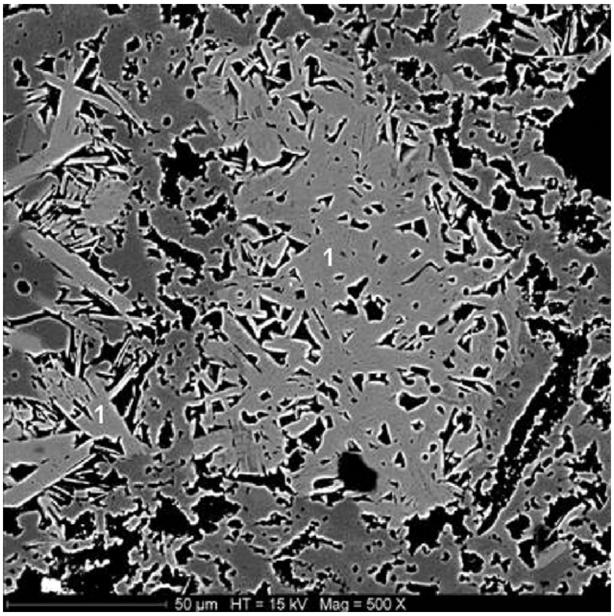

Fig. 7. Calcium hexaluminate (CA_6 - 1) crystals (platelets or needle-like shape) in the matrix of alumina-spinel castables fired at 1500°C..

Additions of even small amounts of silica fume to alumina-spinel castables are detrimental for both thermo-mechanical properties and slag resistance as shown in Figs. 8 and 9. Kriechbaum et al. [29] found a decrease in HMoR at 1500 °C from 17 to 2 MPa when only 0.5% silica fume were added to the alumina-spinel low cement castable. Molin et al. [31] found considerable worse slag resistance of an alumina-spinel castable when compared to alumina-magnesia castables, which can be explained by the small amount of silica fume, which was added to the alumina-spinel castable. The same effect is reported by Ko (Fig. 8) [24].

Spinel addition enhances the thermal shock resistance of alumina castables which can be explained by the different thermal expansion coefficients between alumina and spinel (Table 1). The different expansion leads to microcracks in the matrix that act as crack branchers when the material is thermally stressed. Castables with pre-reacted spinel have proven their good thermal shock resistance in practical applications, for example in purging plugs when cold stirring gas is blown through the hot ceramic. Alumina-magnesia castables show a worse thermal shock resistance when compared to alumina-spinel castables unless the spinel has

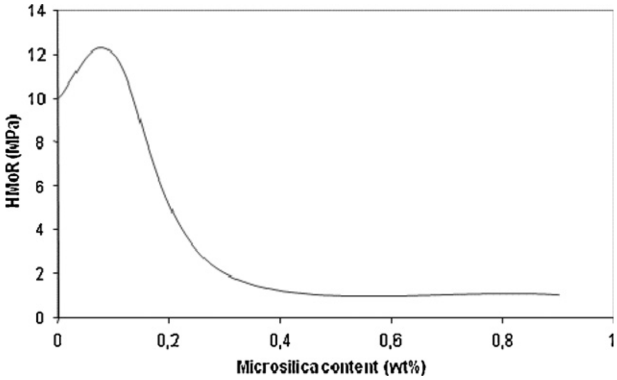

Fig. 9. Effect of silica fume addition on the hot modulus of rupture (HMoR) at 1500°C of alumina-spinel castables [24].

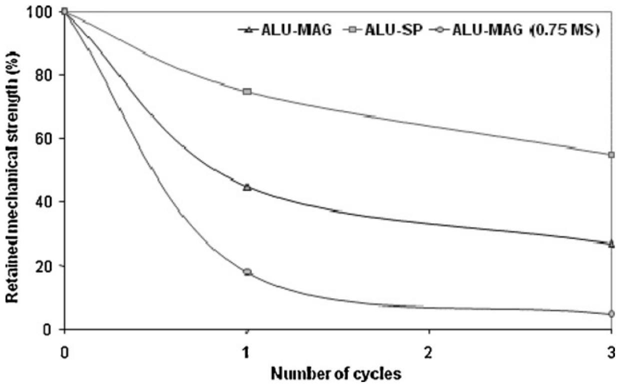

Fig. 10. Mechanical strength change after thermal shock cycles (ΔT = 1100 °C and cooling in water) for ALU-MAG - alumina-magnesia castable, ALU-SP - alumina-spinel castable and ALU-MAG (0.75 MS) - alumina-magnesia castable containing 0.75 wt% of microsilica [32].

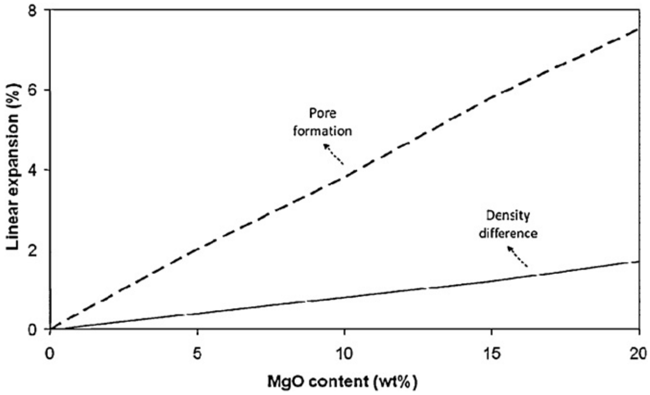

Fig. 12. Linear expansion prediction for distinct MgO contents, considering the difference between the densities of the reactants (MgO and Al_2O_3) and product ($MgAl_2O_4$) or the pores generation mechanism [36].

been formed [28]. Chen et al. [32] found higher mechanical strength retained after thermal shock cycles for alumina-spinel castables compared to alumina-magnesia ones (Fig. 10). However, *in situ* spinel forming castables also provide stress relaxation features, which will be discussed in a later section.

The formulation of castables containing pre-reacted spinel and that of spinel forming alumina-magnesia castables requires different approaches. The use of magnesia as one of the reactants for the spinel formation in castables often causes difficulties such as poor flow or quick setting due to the magnesia hydration. Furthermore, the volume expansion owing to the hydration may lead to cracking during the drying step, which is especially critical when producing pre-cast shapes. The *in situ* formation of spinel is also linked with a relevant volume expansion that needs to be controlled. Too much expansion would lead to mechanical stresses and thus spalling of the lining. This aspect will be discussed in detail in the following section.

3. *In situ* spinel-forming castables

3.1. Mechanism of spinel formation

According to Wagner's mechanism [33], the solid state spinel formation is carried out through the Al^{+3} and Mg^{2+} ions counter-diffusion, at the MgO-$MgAl_2O_4$ and Al_2O_3-$MgAl_2O_4$ interfaces. In order to keep the electro-neutrality, 3 Mg^{2+} ions diffuse to the alumina side, whereas 2 Al^{3+} ions to the magnesia one. Due to this balance of charges, the reaction between 4 MgO and 2 Al^{3+} results in the formation of 1 $MgAl_2O_4$ at the MgO-$MgAl_2O_4$ boundary, whereas 4 Al_2O_3 and 3 Mg^{2+} leads to the generation of 3 $MgAl_2O_4$ at the Al_2O_3-$MgAl_2O_4$ boundary. As a consequence, due to the higher solubility of the Al_2O_3-$MgAl_2O_4$ layer [34], the theoretical thickness ratio (R) between the formed spinel layers at the alumina and magnesia sides is 3:1, indicating a higher spinel formation rate at the Al_2O_3 interface. Additionally, two features help to increase R ratio: (i) the alumina solid solution in spinel and (ii) the MgO vapor transportation. For an intrinsically close contact between magnesia and alumina, a surface diffusion mechanism could also proceed from MgO to Al_2O_3, as the magnesia surface diffusion is higher than the alumina one [33] Considering these aspects, the spinel formation is mostly prone to be carried out at the alumina grains for similar particle sizes of both oxides. Fig. 11 illustrates this counter-diffusion mechanism and, consequently, the higher spinel formation rate at the alumina boundary [33].

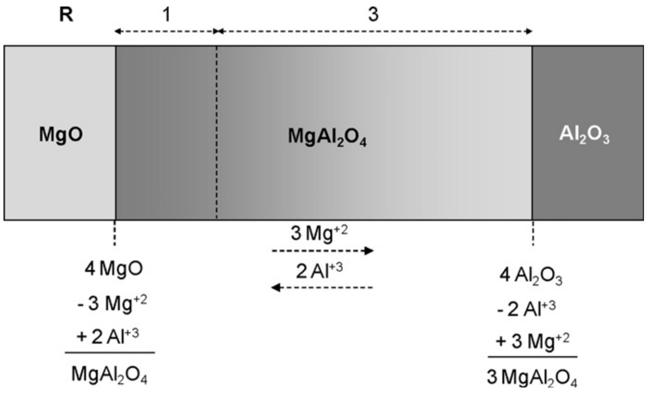

Fig. 11. Spinel formation mechanism through the counter-diffusion of Al^{3+} and Mg^{2+} cations [33].

The *in situ* spinel formation expansive behaviour is commonly attributed to the density differences among the reactants and the product (MgO - 3.58 g/cm^3, Al_2O_3 - 3.98 g/cm^3 and $MgAl_2O_4$ - 3.60 g/cm^3) leading to a volumetric expansion close to 8% and a linear one of 2.6% for an equimolar alumina-magnesia mixture [33,35]. In practice, however, higher expansion values were detected in alumina-magnesia compositions. According to Kiyota [36], the generation of pores after the magnesia diffusion is even more relevant than the density differences among alumina, magnesia and spinel, as shown in Fig. 12. Fig. 13 indicates this phenomenon when MgO diffuses to the alumina grains [36]. Further aspects that affect the spinel expansion, such as the magnesia or alumina grain sizes and the microsilica content will be further discussed in this article.

Regarding the *in situ* spinel grain morphology, it is defined according to its crystalline structure, the crystal's growth conditions and the presence of impurities [37]. Therefore, as

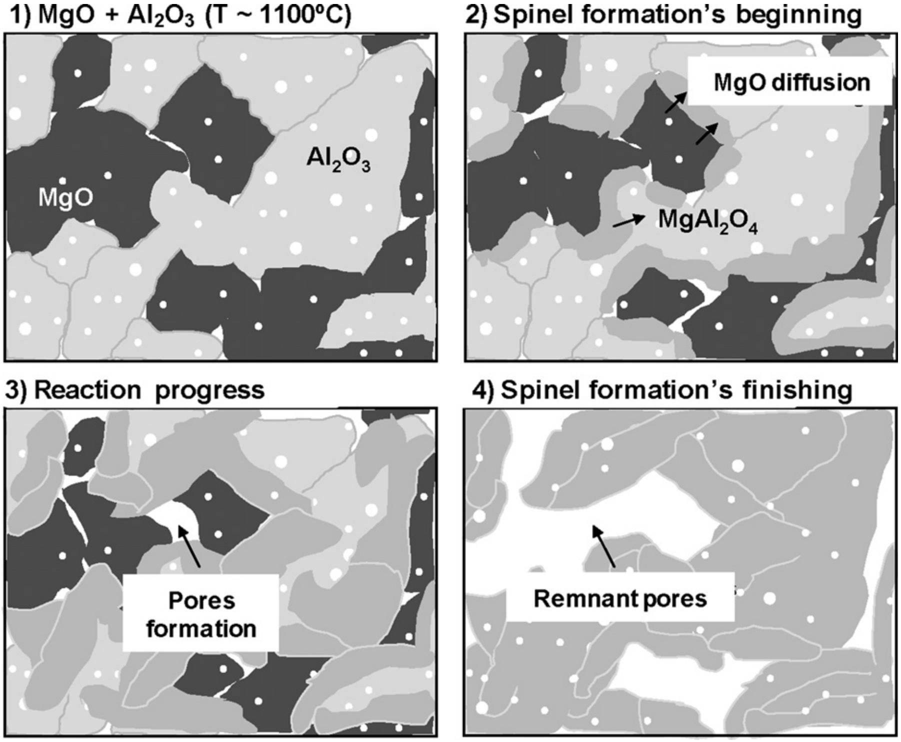

Fig. 13. Pore generation phenomenon due to the Mg^{2+} diffusion [36].

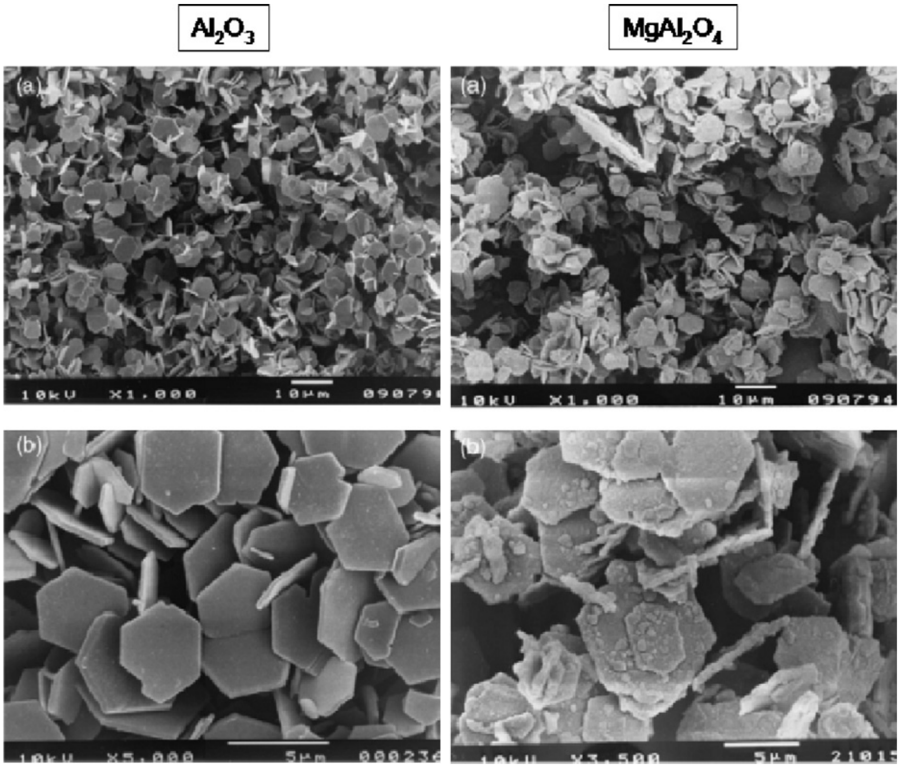

Fig. 14. Template mechanism of the spinel formation [42].

spinel presents a cubic structure, this would be the most thermodynamically stable one, indicating for instance, low likelihood of platelet shaped morphology development [38]. However, the synthesis of acicular spinel crystals has been obtained by an oxide-reduction reaction among magnesia, carbon and aluminum in a CO and CO_2 atmosphere. In this work, $Al_{(g)}$ and $Mg_{(g)}$ were generated by heating a powder mixture of Al+C and MgO + C + Al at 1500 °C under a

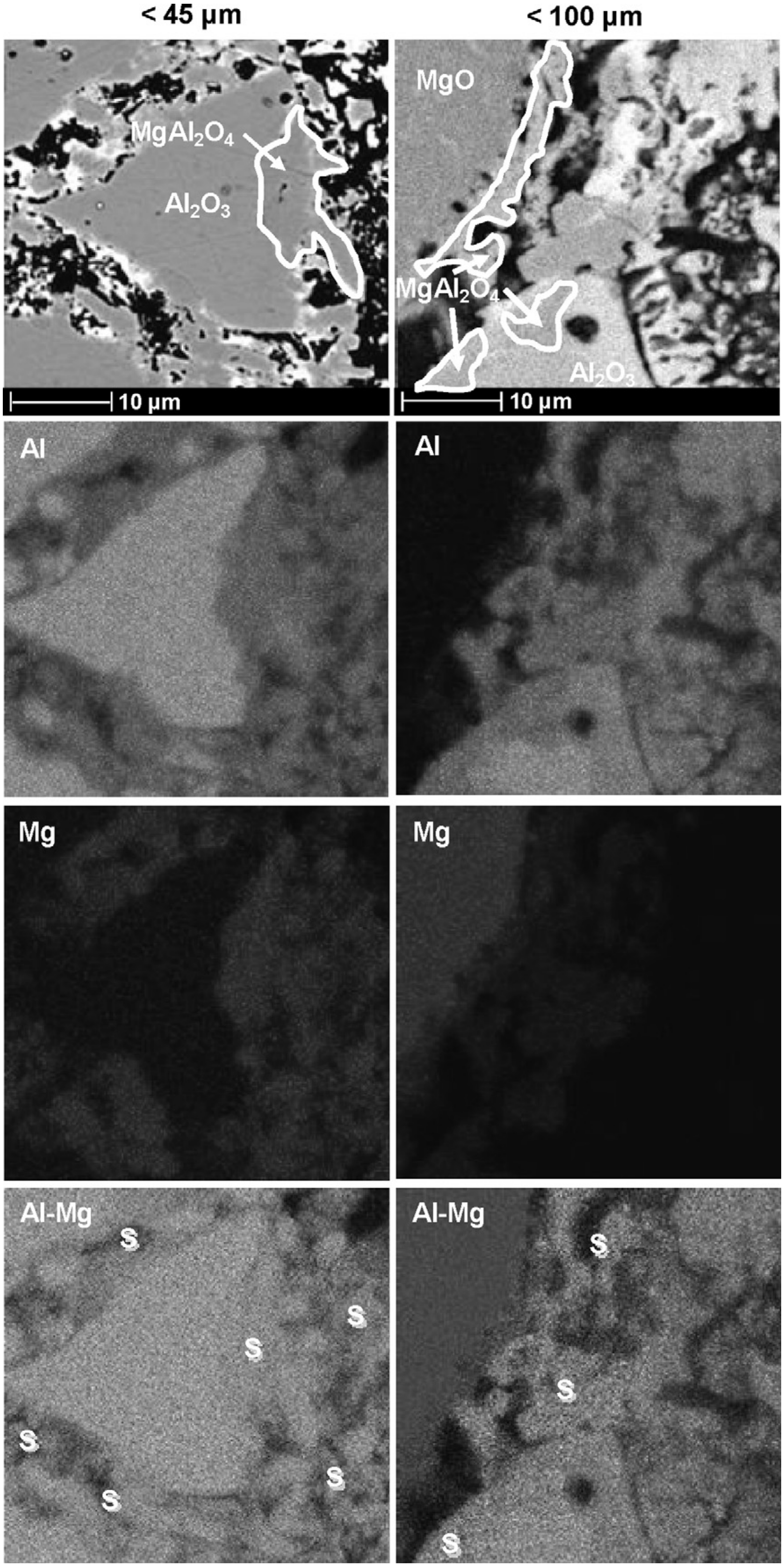

Fig. 15. Spinel formation template mechanism at the edge of alumina or magnesia grains, according to different MgO grain size (< 45 or < 100 μm) [43].

$p_{co} = 0.1$ MPa. Afterwards, the pO_2 was increased by adding CO_2, resulting in the condensation of $Al_{(g)}$ and $Mg_{(g)}$ as spinel whiskers [39].

Previous studies in the literature [40–42] pointed out the production of platelet shaped spinel crystals by using alumina precursors. It should be noted that in polished sections, platelets often appear as needles due to the 2-dimensional view (Fig. 14). This process is called template mechanism, where the formed spinel assumes, to a high extent, the same morphology and size of the alumina precursor. As this mechanism represents the diffusion of the most soluble reactant to the surface of the less one, the spinel formation can also be detected at the edge of magnesia grains, if they present lower specific surface area. This latter situation was detected by Braulio and co-workers [43], when using coarse MgO grain sizes as shown in Fig. 15.

Further parameters that influence the *in situ* spinel formation, morphology and expansion need to be considered. Firstly, it is of the utmost importance to evaluate the effect of the main purity of raw materials on the *in situ* spinel-forming refractory castables: magnesia, alumina and silica fume. Additionally, these castables are commonly bonded with calcium aluminate cement (CAC) and, then two other expansive reactions must be taken into account: the calcium dialuminate (CA_2) and the calcium hexaluminate (CA_6) formation. Thus, before analysing the effect of the usual raw materials on the spinel generation, the influence of CAC will be pointed out.

3.2. Raw materials effect on the expansion behaviour and other properties

3.2.1. Calcium aluminate cement and hydratable alumina

In the literature, the expansion behaviour of alumina-magnesia refractory castables is commonly related to the *in situ* spinel generation. Nevertheless, a previous study [44] reveals that the linear expansion of these castables varies with its calcium aluminate cement (CAC) content (Fig. 16), indicating that it also affects its volumetric stability. According to the literature [45–47], the formation of calcium hexaluminate (CA_6) at temperatures higher than 1450 °C, leads to a theoretical volumetric change of + 3.01% based on the following reaction: $CA_2 + 4\ A = CA_6$.

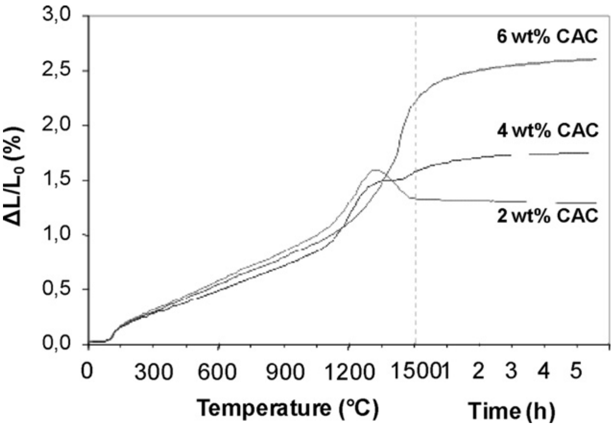

Fig. 16. Expansion behaviour of alumina-magnesia castables containing different calcium aluminate cement (CAC) amounts (6, 4, and 2 wt%) [44].

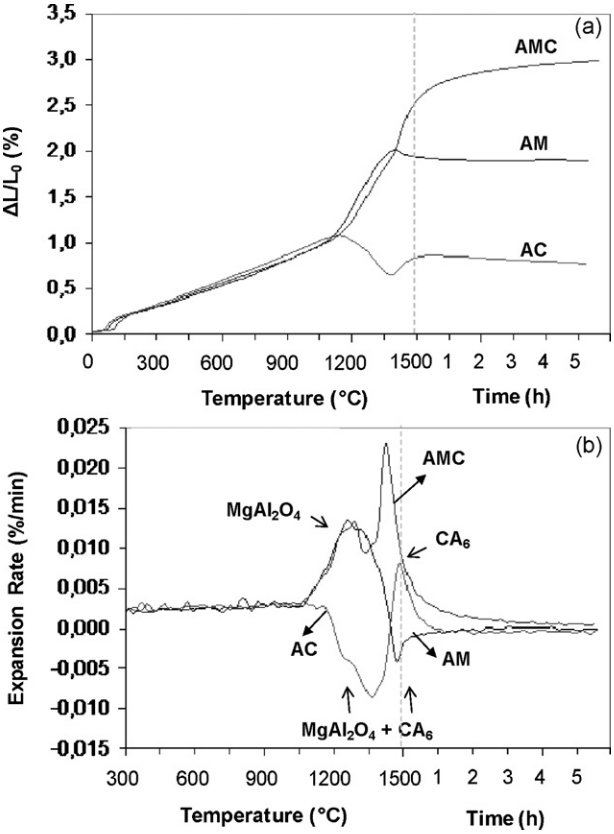

Fig. 17. (a) Expansion behaviour and b) expansion rate of alumina-CAC castable with no MgO (AC), alumina-magnesia castable with no CAC (AM), and alumina-magnesia castable bonded with CAC (AMC) [44].

Therefore, in order to understand the cement role to the overall expansion, three compositions were evaluated: (i) alumina - magnesia - microsilica castable with no CAC (AM), (ii) alumina - CAC - microsilica castable with no MgO (AC) and (iii) alumina - magnesia - microsilica castable containing CAC (AMC). The thermal expansion profiles (up to 1500 °C) of these materials are shown in Fig. 17a [44]. The CAC containing composition (AC) presented the lower linear expansion level (0.8%), whereas the MgO containing one (AM) led to an intermediate expansion (2%). As both systems displayed expansion, when CAC and MgO were added to AMC composition, the result leads to a higher overall expansion (3%).

The spinel and CA_6 expansion rates were then analyzed by the derivative of the expansion curves, resulting in a novel way to follow the progress of both reactions (Fig. 17b) [44]. As the first reaction peak in the alumina-magnesia castable (AM) was close to 1200 °C, it was attributed to the $MgAl_2O_4$ formation. The second one was related to the CA_6 generation, as can be detected in the alumina-CAC castable (AC) at temperatures higher than 1450 °C. Therefore, the overall expansion behaviour of alumina-magnesia castables is dictated, not only by the spinel, but also by the CA_6 generation.

Besides the CA_6 formation, another expansive reaction associated to the cement addition is related to the calcium

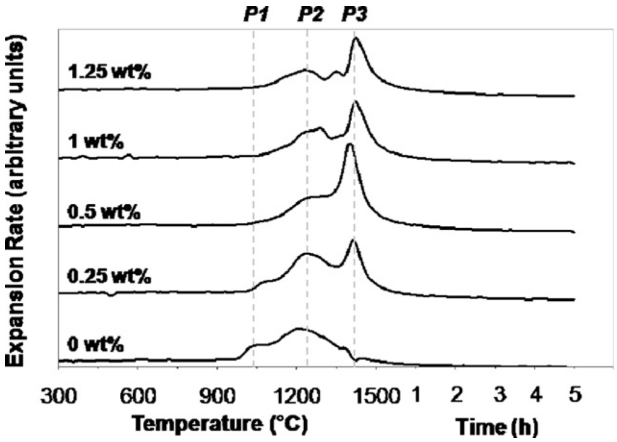

Fig. 18. Expansion rate of alumina-magnesia castables containing different silica fume contents (0, 0.25, 0.5, 1, or 1.25 wt%). The expansion rate peaks P1, P2, and P3 are related to the CA_2, $MgAl_2O_4$, and CA_6 formation, respectively [48].

dialuminate (CA_2) generation ($CA + A = CA_2$), leading to a theoretical volumetric change of +13.6% [45]. Studies conducted by Auvray and colleagues [47] in alumina-cement matrices indicated lower experimental expansion and attributed this result to its better accommodation in the sample pores.

Nevertheless, a further aspect that affects the CA_2 expansion is the castable's silica fume content. A previous study by some of the authors [48] highlighted the presence of another expansion peak when reducing the microsilica content in alumina-magnesia castables, as shown in Fig. 18. This peak was attributed to the CA_2 formation because it occurs in the temperature range around 1000 °C. For the microsilica free composition (0 wt%) or for the one containing only 0.25 wt% of microsilica, there was no competition between silica and alumina to react with calcia, increasing the likelihood of CA_2 formation.

An additional role of silica fume (microsilica) in the calcium aluminate phases is its effect on the CA_6 crystal morphology. Fuhrer and co-workers [49] indicated that acicular-shaped CA_6 crystals are commonly observed as clusters at the surface of tabular alumina grains. Nevertheless, microsilica free alumina-magnesia castables showed equiaxed CA_6 crystal growth instead of the most common platelet shape [48]. Conversely, in the presence of a liquid phase (for a composition containing 0.5 wt% of microsilica), acicular-shaped CA_6 crystals were detected. Fig. 19 summarises the different CA_6 crystal morphologies in the presence or not of liquid phases. This result was in line with those presented by Chen et al. [32], indicating that the well grown platelet shaped CA_6 crystals were not detected in castables without microsilica.

Moreover, as presented by Ko and Lay [50], high permanent volumetric expansion is expected for silica fume containing castables due to the CA_6 crystal growth in the presence of the liquid phase. Regarding this aspect, An and colleagues [51] proposed different CA_6 morphologies (equiaxed or platelet

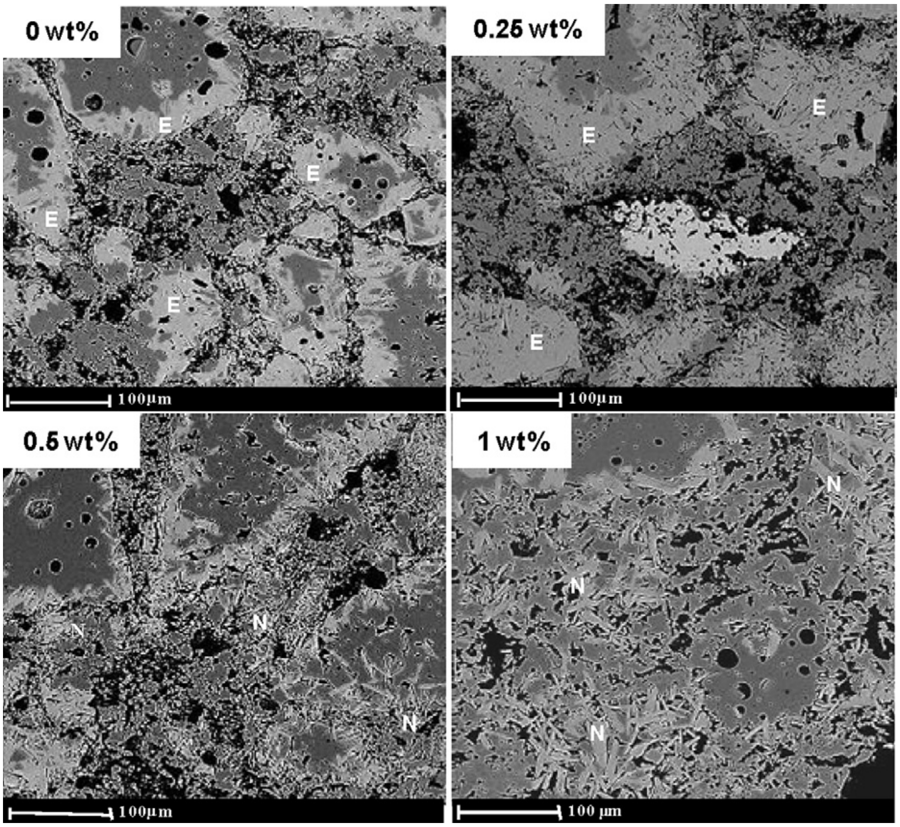

Fig. 19. CA_6 distribution and morphology in alumina-magnesia castables, containing different silica fume contents (0, 0.25, 0.5, and 1 mass %), after firing at 1500°C for 5 hours. CA_6 crystals were detected mainly in an equiaxed morphology (E) for the samples containing 0 and 0.25 mass % silica, whereas platelet shaped ones (N; appear like needles in the 2-dimensional picture) were mostly observed for the castables containing 0.5 and 1 mass % silica [48].

shaped) according to the sort of alumina - calcia reaction mechanism. A high extent of a solid state reaction between alumina and calcium aluminate phases would favour the formation of equiaxial crystals, whereas a solution precipitation reaction would prevail if a previous extensive wetting of the reactant phases is carried out, leading to platelet shaped CA_6 crystals.

The calcium hexaluminate formation also imparts benefits to the alumina-magnesia refractory castables properties [52,53]. When formed with platelet shapes, the CA_6 crystals could enhance the thermal shock and creep resistance and the hot mechanical strength due to the development of toughening mechanisms such as crack deflection and bridging [54]. Furthermore, its rather low solubility in high-iron containing slag should increase the corrosion resistance of the castables.

However, when designing the overall expansion of a spinel forming castables, the CA_6 generation and consequently the CAC content needs to be carefully considered. According to Braulio et al. [44] an intermediate cement content (4 wt%) would be the most suitable solution, for a simultaneous optimisation of the expansion behaviour and the thermo-mechanical properties, with a well-designed CA_6 development. A further alternative is the use of a high-alumina containing cement (80 wt% instead of the usual 70 wt% one) [55].

In addition, castables containing hydratable alumina binder provide an alternative to the cement bond. They can inhibit the potential drawbacks associated with the CA_6 formation [56,57]. The withdrawal of CaO out of the system when replacing CAC by hydratable alumina can also improve the hot properties of alumina-magnesia castables [58]

The reduction in the CAC content and addition of hydratable alumina led to lower linear expansion levels, as presented in Fig. 20 [56]. In this work, compositions containing only CAC (6 wt% - 6C) or hydratable alumina (6 wt% - 6H) were compared with those adding both binders (2 wt% CAC + 4 wt% hydratable alumina - 2C4H or 4 wt% CAC + 2 wt% hydratable alumina - 4C2H). A noteworthy reduction in the overall expansion was detected by the replacement of CAC by hydratable alumina. The use of this binder also affected the spinel formation, as will be discussed in a later section.

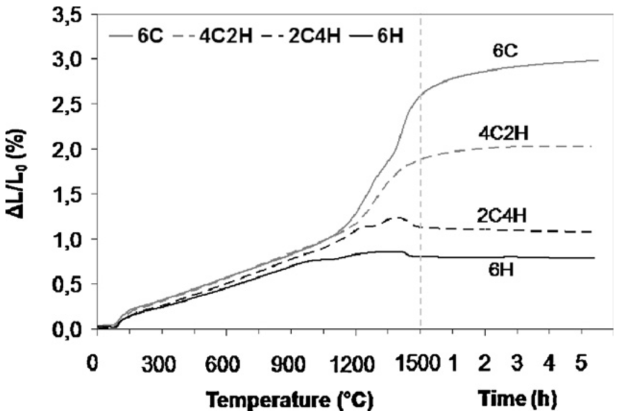

Fig. 20. Expansion behaviour of alumina-magnesia castables containing 6 wt% CAC (6C), 4 wt% CAC + 2 wt% HA (4C2H), 2 wt % CAC + 4 wt% HA (2C4H) or 6 wt% HA (6H) [56].

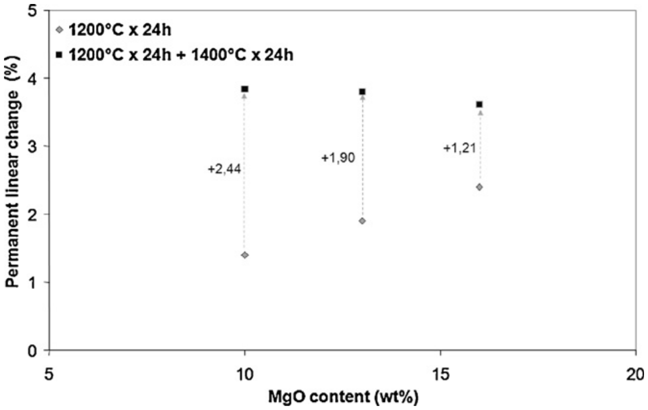

Fig. 21. Relationship between the MgO content and the permanent linear change for a dual sintering process (1200 and 1400°C) [59].

Fig. 20 - Expansion behaviour of alumina-magnesia castables containing 6 wt% CAC (6C), 4 wt% CAC + 2 wt% HA (4C2H), 2 wt % CAC + 4 wt% HA (2C4H) or 6 wt% HA (6H) [56].

Besides the CAC content, also the magnesia one and the grain size can affect the CA_6 generation. Considering that *in situ* spinel formation takes place before the CA_6 generation, Ide and co-workers [59] performed a two-step sintering test: a first firing at 1200 °C for 24 hours (inducing the spinel generation), followed by a second at 1400 °C for 24 hours (leading to the CA_6 formation). This test was conducted with different MgO contents or grain sizes and the permanent linear change (PLC) of the samples was evaluated after each firing. The purpose of this test was to investigate the amount of expansion related to the CA_6 formation at the 1400 °C firing, after the consumption of the fine alumina particles needed to carry out the spinel reaction.

Fig. 21 illustrates the result obtained for different MgO amounts [59]. After firing at 1200 °C, the PLC values are proportional to the MgO content or the amount of spinel being formed. The same samples were then fired at 1400 °C and the PLC decreased for higher magnesia amounts. Therefore, increasing the MgO content resulted in a higher consumption of fine alumina, restraining the CA_6 formation afterwards, and leading to a higher CA_6 formation at the border of tabular alumina grains. Sako and colleagues [60,61] also found this behaviour where *in situ* spinel castables consume part of the fine alumina from the matrix, thus inducing the CA_6 generation at the edge of tabular alumina grains.

An increase in MgO grain size leads to an opposite effect, and the difference in PLC between the first and second firing becomes higher (Fig. 22) [59]. This reaction is mostly relevant after the second firing because higher MgO grain sizes delay the start of spinel formation. Furthermore, the CA_6 formation rate increases when a higher amount of fine alumina is available.

3.2.2. Magnesia

A key issue for designing alumina-magnesia castables is the selection of the MgO source as this raw-material affects several processing steps, such as shaping, curing and drying [62–64].

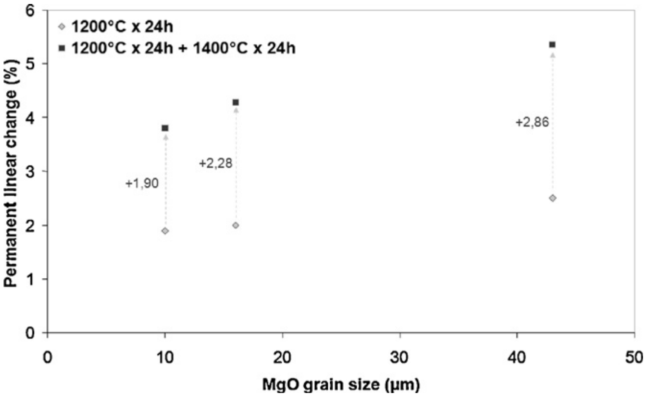

Fig. 22. Relationship between the MgO grain size and the permanent linear change for a dual sintering process (1200 and 1400°C) [59].

The magnesia grain size, purity and reactivity influence, for instance, the MgO hydration and also the spinel formation.

The impurities commonly detected in dead-burnt magnesia are silica, calcia, iron oxide, alumina and boron oxide. These impurities react with MgO or among each other, leading, for example to distinct lime or lime-magnesia silicates. According to Landy [65], the CaO/SiO_2 wt. ratio (C/S) determines the formation of additional phases: high CaO content (ratio > 2.8) results in tricalcium silicate (Ca_3SiO_5) and free CaO, whereas high SiO_2 amount (ratio < 0.93) leads to monticellite ($CaMgSiO_4$) and forsterite (Mg_2SiO_4). This ratio also affects the properties at high temperatures: when the SiO_2 content increases (lower CaO/SiO_2 ratio), the initial melting temperature of MgO particles decreases (from 1850 °C for high CaO contents to 1500 °C for high SiO_2 amounts) [65,66].

The C/S ratio and the MgO purity both affect the *in situ* spinel formation. Nevertheless, this takes place indirectly, as both higher CaO/SiO_2 ratio and magnesia purity results in higher brucite ($Mg(OH)_2$) content and, therefore, enhance the magnesia chemical activity during sintering leading to an increase in the spinel reaction driving force [67].

Considering this aspect, the use of coarse MgO grains would be a suitable way to inhibit the MgO hydration as it is a surface-controlled effect. However, the increase in the magnesia grain size affects the spinel formation, reducing its content and leading to a higher overall expansion. Moreover, if some coarse MgO grains remain unreacted, cracks could be generated during thermal cycling, due to the thermal expansion mismatch among magnesia, alumina and spinel [23,35,67].

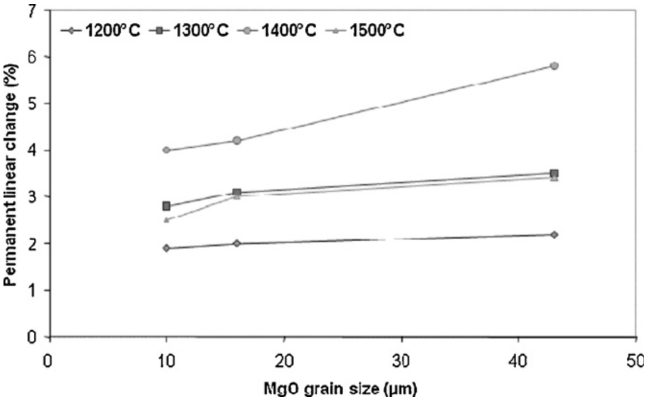

Fig. 23. MgO grain size effect on the permanent linear change of alumina-magnesia castables [68].

Regarding the expansion behaviour, coarse magnesia grain sizes result in higher expansion as shown in Fig. 23 [59]. This aspect could be associated with the generation of large pores during spinel formation, due to the Mg^{2+} diffusion, according to Nakagawa [33] and Kiyota [36]. Considering this phenomena, the use of ultra-fine MgO grain sizes (micronized below 13 µm and nano powder - average particle size close to 20 nm) was evaluated in order to reduce the expansion and the starting temperature of the spinel formation [68].

Fig. 24 shows the expansion profile and the expansion rate as a function of temperature and time of alumina-magnesia castables containing 6 wt% of dead-burnt MgO with different grain sizes ($<$ 100, $<$ 45 or $<$ 13 µm or nano) or a mixture between 3 wt% of nano MgO and 3 wt% of MgO $<$ 45 µm [68]. Due to the increase in the specific surface area, the starting temperature of spinel formation was reduced from 1200 °C to 1000 °C, when changing from coarse MgO ($<$ 100 µm) to nano-scaled magnesia, according to the spinel expansion rate peak (Fig. 24b). In addition an outstanding reduction of the overall expansion was obtained (Fig. 24a) when decreasing the MgO grain size. This indicates an alternative for attaining higher volumetric stability and better corrosion resistance due to finer dispersed spinel in the matrix of the castable.

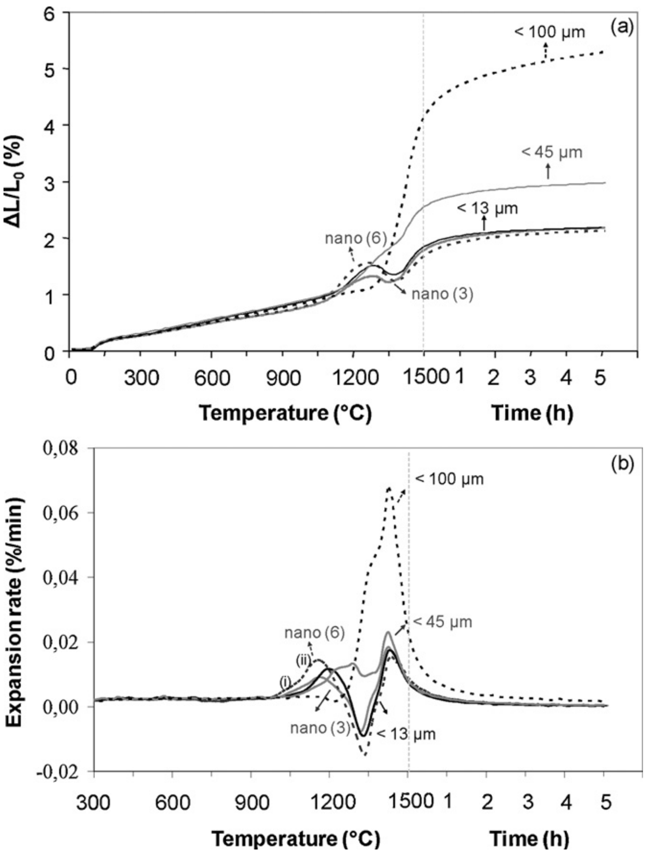

Fig. 24. (a) Expansion behaviour and (b) expansion rate of alumina-magnesia castables containing different MgO grain sizes [68].

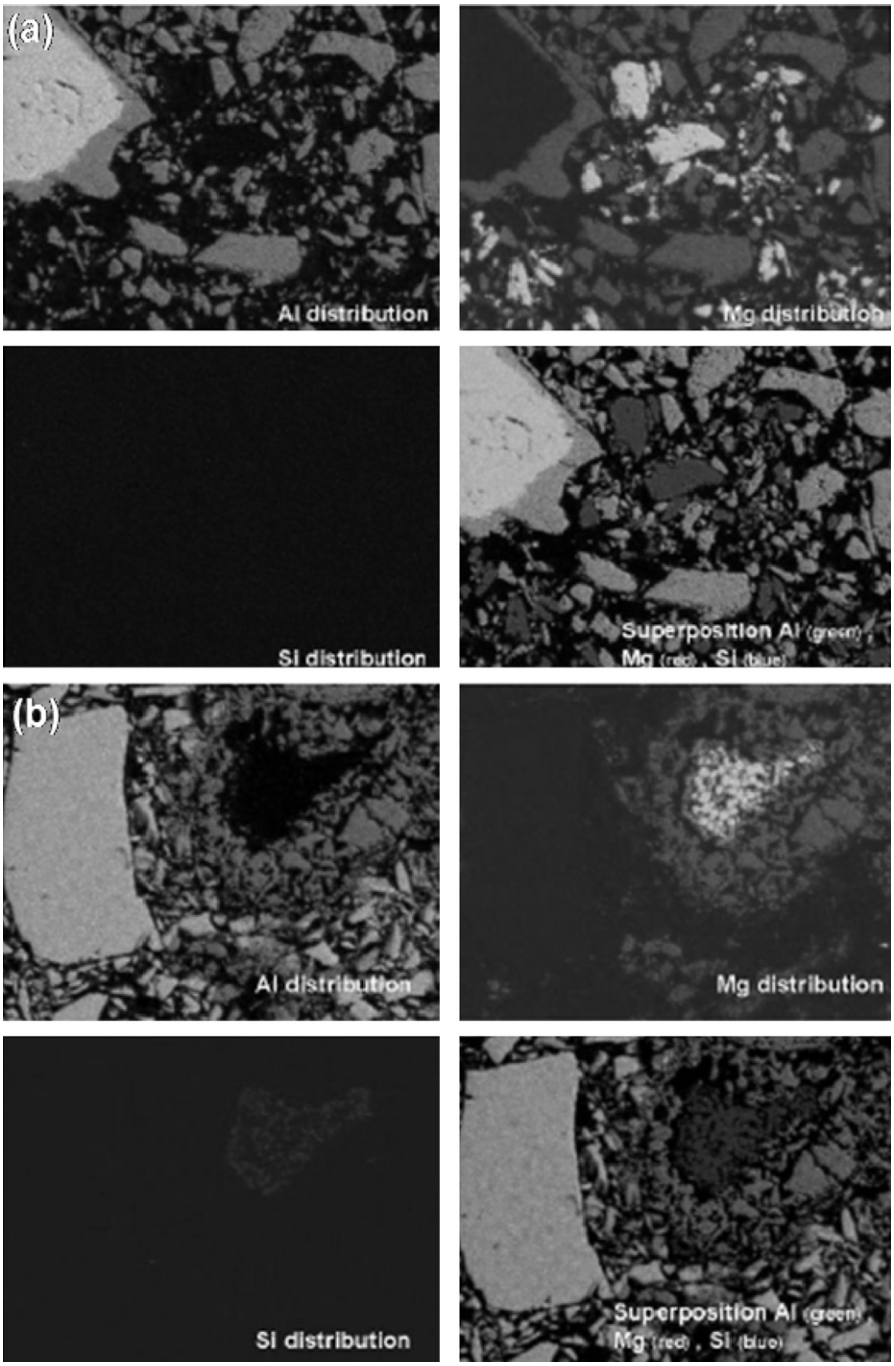

Fig. 25. Spinel formation at the edge of alumina or magnesia grains, for (a) fine MgO grain sizes or (b) coarser MgO grain sizes [67].

Concerning the nano MgO powder addition, the mixture named nano (3) led to the lowest spinel expansion level. Nevertheless, the expected spinel expansion reduction for the alumina-magnesia castable containing only nano magnesia (nano (6)) was not achieved because it was not possible to avoid the agglomeration of MgO nano particles. These agglomerates act in the same way as coarser magnesia particles would do. Therefore, the challenge will remain to fully disperse nano powders into refractory castables before the noteworthy advances highlighted in the literature for the nano spinel powder production could be attained [69–74].

A further aspect associated with the MgO grain size is the mechanism of spinel generation itself. When using fine MgO grain sizes, spinel is formed mainly by Mg^{+2} diffusion into alumina grains [43], whereas the use of coarser MgO grains results in the spinel formation at the edge of MgO particles, involving Al^{+3} diffusion. Fig. 25 shows the different spinel template mechanisms as evaluated by Soudier [67]. Mori and colleagues [75] also detected by X-ray diffraction of alumina-magnesia compositions fired at 1200 °C that the periclase peak decreased when coarser alumina grains were used, whereas the use of coarse MgO grains led to the consumption of corundum.

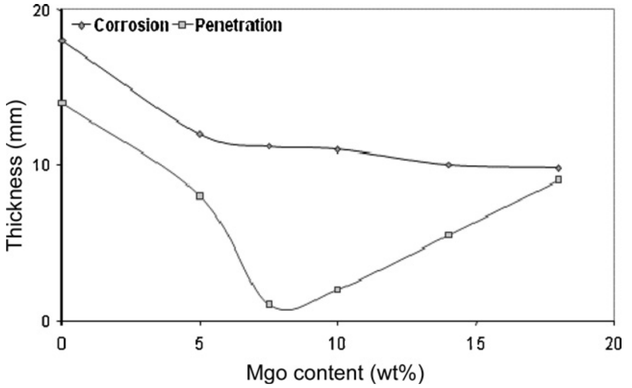

Fig. 26. Effect of MgO content in alumina-magnesia castables on the corrosion and slag penetration resistance [79].

In Fig. 25, a high silica concentration at the MgO grains can be observed for the coarser MgO composition. According to Sarpoolaky [76], alumina-magnesia castables presented a forsterite (Mg_2SiO_4) layer after sintering at 1400 °C, making the alumina-magnesia reaction progress more difficult. Myhre and co-authors [77] indicated that this phase is formed at temperatures above 1100 °C and followed by shrinkage. Cunha-Duncan and Bradt [78] also studied such a reaction and concluded that forsterite formation is even more favourable than the spinel one, from a thermodynamic standpoint.

The content of magnesia added to the *in situ* spinel castables compositions affect their properties, due to the changes in the amount of spinel generated. Studies carried out by Tawara et al. [79] indicated an optimal MgO content in the range of 5 to 10 wt% (Fig. 26). Above these values, the slag infiltration resistance is deteriorated, due to the massive spinel formation and consequently cracking of the material. This magnesia content range is in line with the already discussed optimal spinel content range of 15-30% for slag corrosion and penetration resistance of alumina-spinel castables. Molin and colleagues [31] reported the best results in a crucible slag test for *in situ* spinel castables containing 2.5 or 5 wt% MgO (Fig. 27).

3.2.3. Alumina

Jono and co-workers [80] concluded by XRD analyses that the reduction of its grain size results in faster spinel formation at lower temperatures, lower linear expansion and higher shrinkage after sintering. Nevertheless, the use of an ultra-fine alumina could cause peeling if a high shrinkage takes place. Zargar et al. [81] evaluated the addition of nano boehmite on the spinel formation. It resulted in the development of a homogeneous microstructure, which could enhance the ability for controlling the *in situ* spinel expansion.

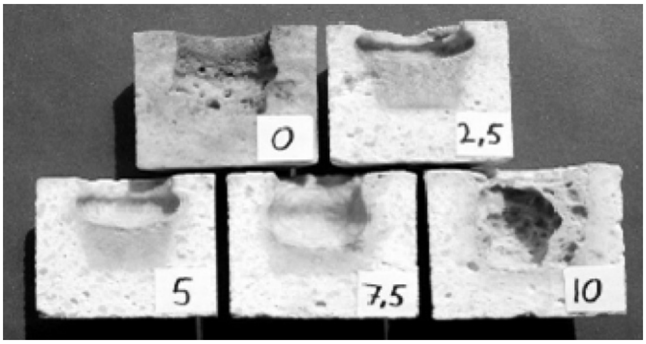

Fig. 27. Alumina-magnesia castables containing different MgO amounts from 0 to 10 wt% after crucible slag test (CaO:SiO2 =2.6, 1650°C, 4 hours) [31].

The factors to be considered in the investigation are the content of fine aluminas, their mineralogical phases, their particle size distribution, the dispersion in the castable and reactions with other castable compounds than magnesia.

Given magnesia contents of below 10%, there will always be sufficient alumina available for a quantitative spinel formation. However, the spinel generation rate at lower temperatures depends on the content of fine and ultra-fine aluminas in the castable matrix because their reactivity is higher when compared to the alumina aggregate.

Volume expansion during the spinel formation depends on the alumina precursor phase [82]. Corundum (α-Al_2O_3) has a higher density (3.99 g/cm^3) when compared to Periclase (MgO, 3.58 g/cm^3) and Spinel (3.58 g/cm^3), and therefore results in a high volume expansion during the spinel formation. γ-Al_2O_3 has the spinel crystal structure and a lower density (3.2 g/cm^3), and therefore shows lower expansion. Another transition alumina, ρ-Al_2O_3, showed an intermediate behaviour (Fig. 28). Technically γ-Al_2O_3 is not an option as a fine milled powder in a castable because it is much more difficult to grind when compared to α-Al_2O_3. Therefore γ-Al_2O_3 is not used for spinel forming castables because they would show very high water demand and poor flow properties.

ρ-Al_2O_3 has hydraulic properties and a special grade can be used as binder (hydratable alumina). It is often used as an alternative to calcium aluminate cement especially for spinel forming castables. Fig. 29 presents the expansion rate of castables bonded with calcium aluminate cement or hydratable alumina or mixtures of both binders [56]. Instead of the two well defined expansion peaks detected for the CAC-containing composition (6C), the addition of hydratable alumina led to the reduction of both spinel and CA_6 peaks, as a consequence of sintering and lower CA_6 generation.

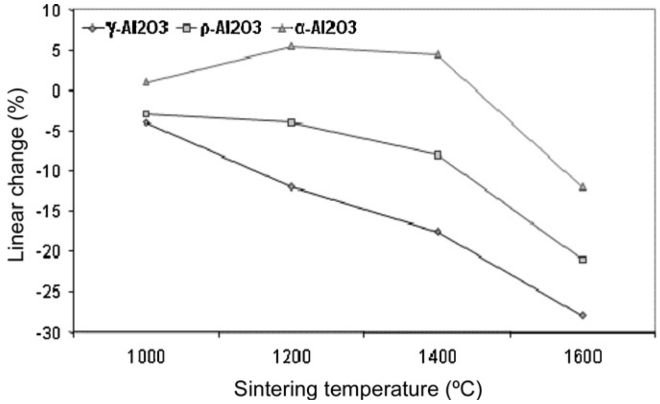

Fig. 28. Linear change of alumina-magnesia samples for different sintering temperature and alumina precursor phases (α, γ and ρ) [82].

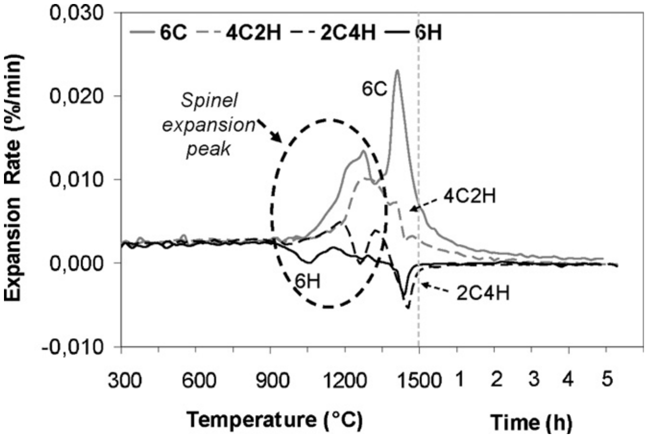

Fig. 29. Expansion rate of alumina-magnesia castables containing 6 wt% CAC, 4 wt% CAC + 2 wt% HA (4C2H), 2 wt% CAC + 4 wt% HA (2C4H) or 6 wt% HA (6H) [56].

In order to further evaluate the hydratable alumina effect on the spinel expansion rate reduction, the following compositions were investigated: a hydratable alumina (6 wt%)-bonded alumina castable (HAC - MgO free), an alumina-magnesia (6 wt%) castable (ISC - *in situ* spinel castable - binder free) and a hydratable alumina (6 wt%)-bonded alumina magnesia (6 wt%) castable (6H). All of them contained 1 wt% microsilica [56] and the results are shown in Fig. 30. Other than CAC containing castables, which display a remarkable expansive behaviour (Fig. 16), hydratable alumina-bonded castables shrink and therefore counterbalance the *in situ* spinel expansion. One of the main reasons for this hydratable alumina sintering behaviour is the formation of a metastable SiO_2-Al_2O_3 liquid close to 1250 °C, leading to the densification of systems containing hydratable alumina and microsilica [83].

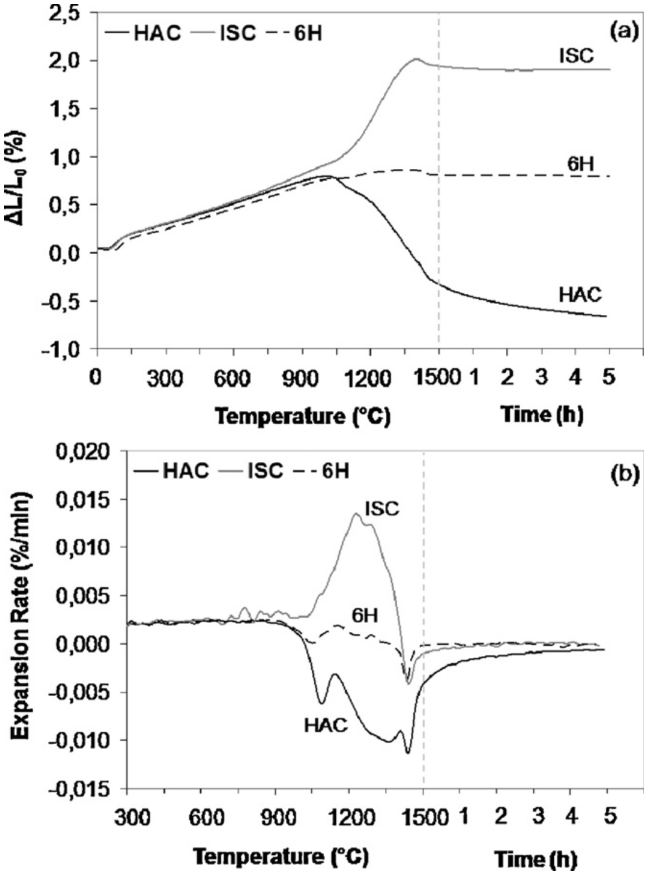

Fig. 30. (a) Expansion behaviour and b) expansion rate of the hydratable alumina-bonded castable with no MgO (HAC), the alumina-magnesia castable with no binder (ISC), and the alumina-magnesia castable containing hydratable alumina (6H). All castables contained 1 wt% of microsilica. [56].

Technically, calcined or reactive aluminas are typically used in the matrix of spinel forming castables. They differ in the average particle size and the specific surface area. A bimodal reactive alumina with d_{50} of 2.5 μm and specific surface area 3 m^2/g was used in this study as standard matrix alumina (CL370). Other alumina raw materials such as nano alumina powder and colloidal alumina, which provide a much higher specific surface area and sintering reactivity, have been discussed in the literature [84,85]. As a novel alternative to induce sintering at lower temperatures, stable nano-scaled alumina dispersions with high solid concentrations present a certain potential to lower the self-agglomeration drawbacks commonly detected in nano powders [86,87].

Fig. 31 shows the impact of different high surface area aluminas on the expansion behaviour of alumina-magnesia castables. The addition of alumina powders with very high surface areas (nano alumina powder - NAP, hydratable alumina - HA and colloidal alumina - CA) resulted in lower overall linear expansion levels when compared to the reference containing a bimodal reactive alumina (REF). Among all compositions, the one containing colloidal alumina presented the lowest expansion and the highest delay on the starting expansion temperature due to its higher sintering effectiveness. Similarly to the nano MgO evaluation discussed before, the use of nano alumina powder resulted in low spinel expansion accommodation ability. Moreover, the hydratable alumina containing castable presented lower overall expansion level when compared to the nano alumina powder castable. This is another example that the benefits of adding nano powders would only be feasible if suitable dispersion can be attained.

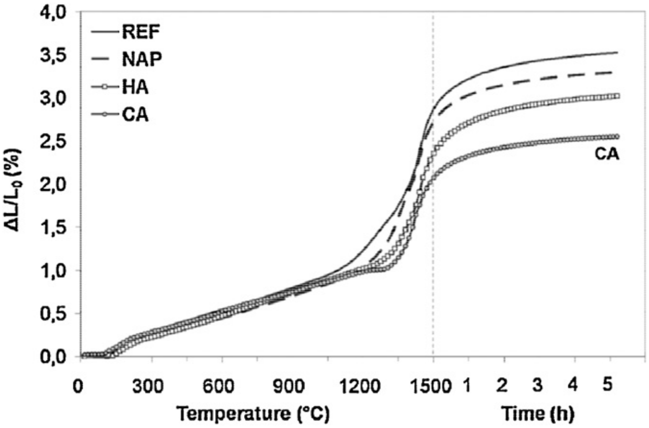

Fig. 31. Expansion behaviour of alumina-magnesia castables containing different fine reactive aluminas. Reference castable with reactive alumina CL370 (REF), others contain mixtures of CL370 with either nano alumina powder (NAP), or hydratable alumina (HA), or colloidal alumina (CA). All castables contain 1% microsilica [84].

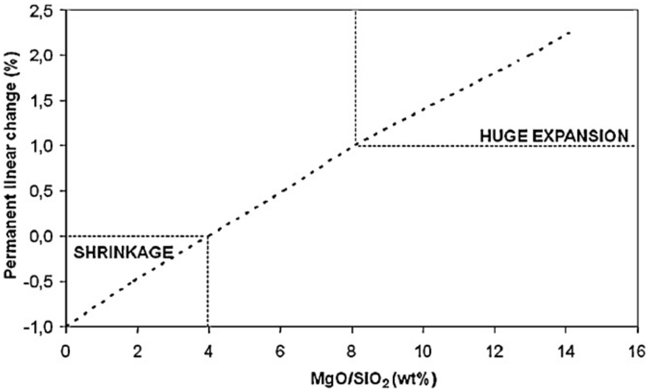

Fig. 32. MgO/SiO_2 wt% ratio effect in the permanent linear change of alumina-magnesia castables [79].

The high price of commercially available nano alumina products shall be also considered.

3.2.4. *Silica fume*

Silica fume plays several roles in alumina-magnesia refractory castables. Due to its ball-bearing effect associated with its spherical shape, the fumed silica addition can increase the castables' flowability [88,89]. Furthermore, this raw material can reduce the MgO hydration rate [90] by forming a magnesium-silicate-hydrate [91,92].

For the *in situ* spinel generation, silica fume can counter-balance its expansion by a softening mechanism. This effect is attained by the formation of low-melting temperature phases, such as gehlenite ($Ca_2Al_2SiO_7$ - C_2AS) or anorthite ($CaAl_2Si_2O_8$ - CAS_2) for CAC-bonded compositions [93]. Therefore, the expansive behaviour of this sort of castable depends on the content of liquid phase, which is directly related to the amount of silica fume added to the composition [48].

According to Tawara and co-authors [79], a high MgO/SiO_2 wt% ratio (> 12) in the castable matrix is detrimental resulting in high permanent linear changes (> 2%) and therefore huge expansion leading to cracking of the material. On the other hand, industrial results indicated that low MgO/SiO_2 wt% ratio (< 3) is not suitable due to a high shrinkage and also cracking generation. Therefore, a suggested MgO/SiO_2 wt% ratio would be between 4 and 8. Fig. 32 correlates the permanent linear change and the MgO/SiO_2 wt% ratio in the castable matrix pointing out that lower values lead to shrinkage, whereas higher values result in huge expansion.

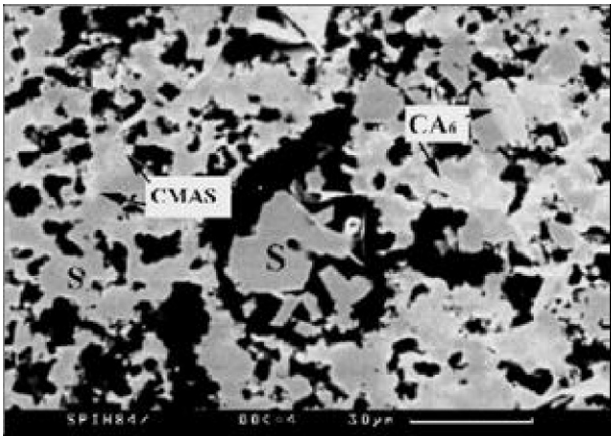

Fig. 33. SEM image of an Al_2O_3-MgO castable fired at 1400°C: detection of spinel (s), CA_6 and CMAS phases [49].

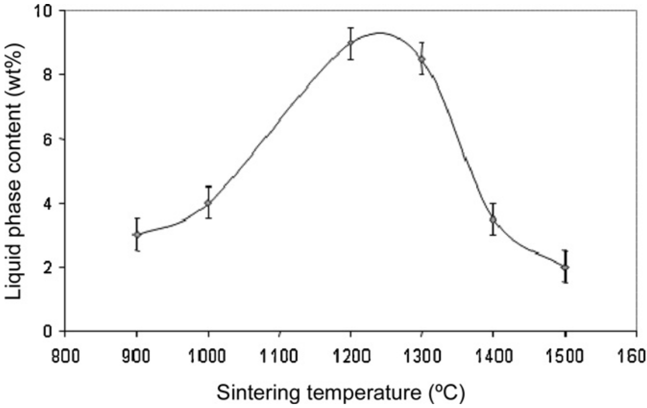

Fig. 34. Liquid phase content in the range of 900-1500°C [46].

Besides the feasible silica fume softening mechanism effect, the liquid phase could also speed up the spinel formation, increasing the Mg^{+2} and Al^{+3} ions diffusion [94,95]. In addition to the ternary eutetics in the Al_2O_3-CaO-SiO_2 and CaO-MgO-SiO_2 equilibrium systems, SEM analyses [49,76] indicated the formation of phases in the CaO-MgO-Al_2O_3-SiO_2 (CMAS) system located close to spinel grains, as shown in Fig. 33. Nevertheless, these quaternary phases were not detected in some other studies [96–98].

Despite its high amount of liquid phase generated by the silica fume addition up to 1300 °C, increasing the firing temperature to 1400 and 1500 °C results in a reduction of its content. This aspect is a consequence of the calcium hexaluminate formation (CA_6) consuming a significant amount of alumina and lime previously in the liquid phase. In order to illustrate this effect, Fig. 34 indicates the amorphous phase evolution as a function of temperature for a high-alumina castable containing 10 wt% of preformed spinel, besides silica fume and calcium aluminate cement. Even in the absence of free MgO, the Al_2O_3-CaO-SiO_2 ternary system leads to the

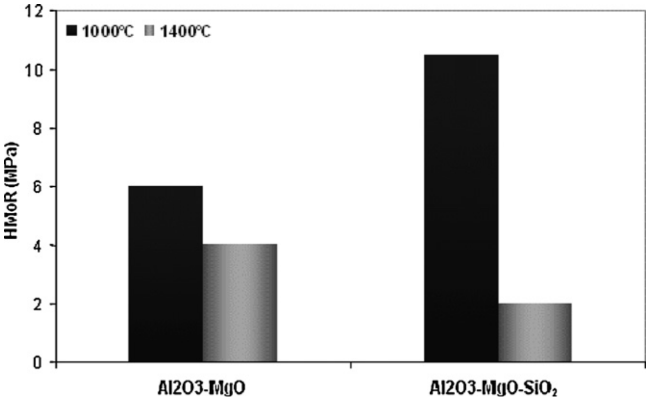

Fig. 35. Hot modulus of rupture (HMoR) at 1000 or 1400°C for alumina - magnesia castables with or without microsilica [99].

formation of a primary liquid phase at 1170 °C. Considering this behaviour, an increase in the transient liquid phase content is detected in the temperature range of 900-1300 °C, followed by its reduction as the CA_6 formation begins [46].

Despite the liquid phase content reduction as the firing temperature is increased, the residual liquid can deteriorate the castableś hot properties, such as the hot modulus of rupture and creep resistance [48,99]. In Fig. 35, a higher decrease in the HMOR from 1000 °C to 1400 °C is detected for a silica fume-containing (0.75 wt%) alumina-magnesia castable composition than for a silica fume-free one [99]. Additionally, research conducted by Shirama and colleagues [100] indicated better corrosion resistance for the lowest microsilica content evaluated (1 wt% from a range between 1 - 3 wt%). According to these authors, lower silica fume amounts result in better corrosion and spalling resistance, due to a lower cracking likelihood. Nevertheless, chemical interactions could not be disregarded, indicating room for further studies in this subject.

The microsilica content also affects the overall expansion of alumina-magnesia refractory castables. For fine magnesia grain size (< 45 μm), microsilica counterbalanced the *in situ* spinel expansion (as commonly stated in the literature) [48]. Fig. 36 presents the expansive behaviour of CAC-bonded alumina-magnesia castables containing different microsilica amounts. Compared to the reference (0 wt% microsilica), lower silica contents (0.25 or 0.5 wt%) led to higher linear expansion levels (Fig. 36a), whereas further microsilica addition (1 and 1.25 wt%) decreased the overall expansion due to higher liquid phase generation, lower CA_6 formation and as a consequence of the softening effect on spinel expansion. Furthermore, a noteworthy reduction in the spinel expansion rate peak was detected when increasing the microsilica content (Fig. 18), indicating a softening mechanism effect during the spinel formation [48].

Conversely, when using a coarser MgO grain size (< 100 μm), the overall expansion increase scaled-up with the microsilica content (Fig. 37a) [101]. According to the upper linear expansion limit for the fine MgO grain size (< 45 μm) [48], shown as a dotted line in Fig. 36a, only the silica free composition was in the same expansion range. Regarding the expansive reactions involved in alumina-magnesia refractory castables, the spinel one was the most affected by the microsilica content as indicated by the derivative of the expansion curves (Fig. 37b) [101]. For this condition, microsilica speeds up the Mg^{2+} dissolution, pointing out that it does not always counterbalance the *in situ* spinel expansion. Therefore, a strict criterion should be used when selecting the silica fume content, as it affects the castables' hot properties, the volumetric stability and the reaction rates of the expansive phases generated during the sintering of *in situ* spinel-forming castables.

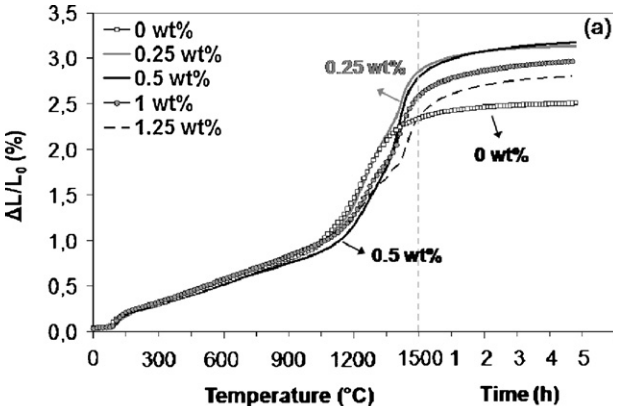

Fig. 36. Expansion behaviour of alumina-magnesia castables containing different microsilica contents (0, 0.25, 0.5, 1 or 1.25 wt%) and MgO < 45 μm [101].

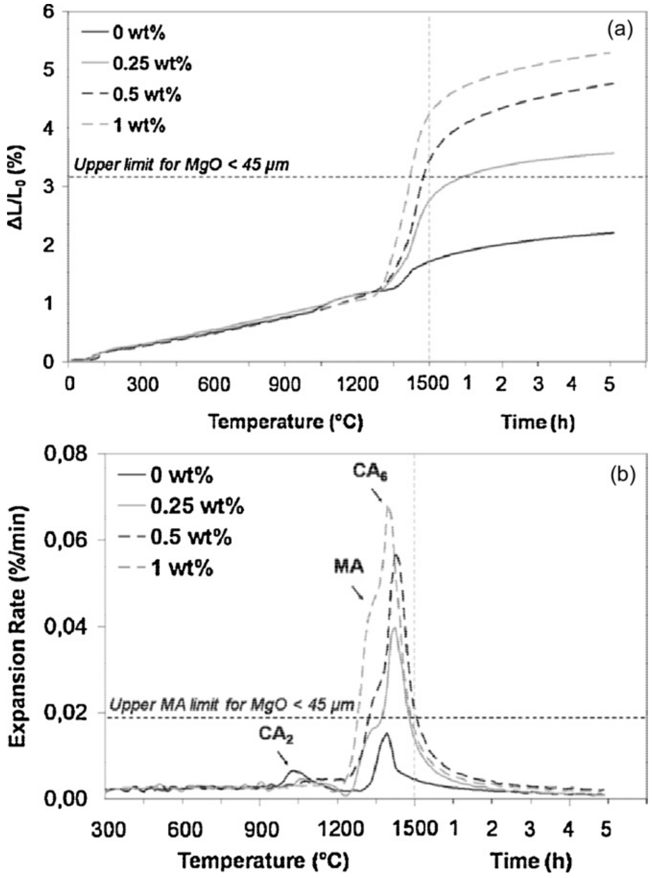

Fig. 37. (a) Expansion behaviour and (b) expansion rate of alumina-magnesia castables containing different microsilica contents (0, 0.25, 0.5, 1 or 1.25 wt%) and MgO < 45 μm. MA: $MgAl_2O_4$ [101].

4. Preformed and *in situ* spinel in steel ladle applications

Preformed and *in situ* spinel castables could be very similar with regards to the data typically provided on technical data sheets of refractories such as the chemical composition and bulk density. However, the previously discussed properties show distinct differences between the two concepts which are important for applications in the steel ladle [102], as shown in Fig. 38. This has been discussed in more detail by Schnabel et al. [103] recently.

Preformed alumina-rich spinel containing castables show volumetric stability and high mechanical strength at steel

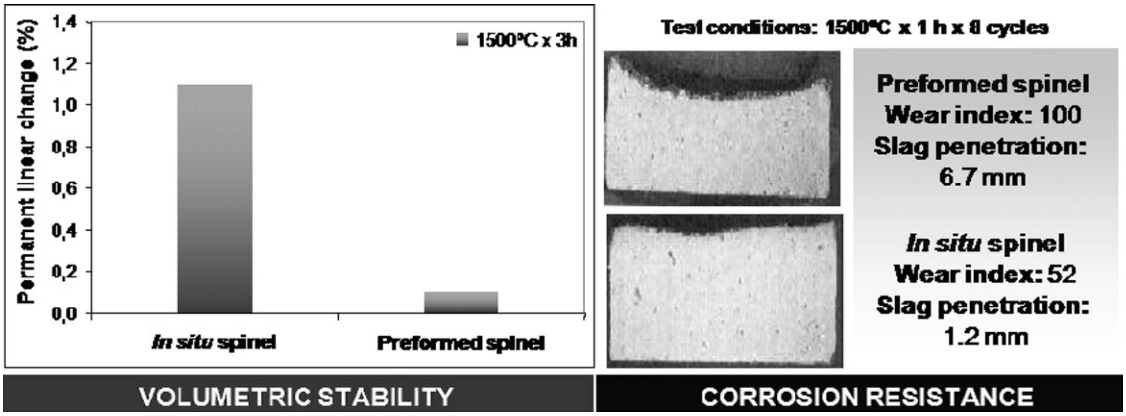

Fig. 38. Advantages and drawbacks of preformed and *in situ* spinel-containing castables [102].

making temperatures (HMoR, RuL). They also have a higher thermal shock resistance and slag resistance when compared to pure alumina refractories. It is important to mention that no silica fume addition is required in these castables and that it should not be used because of the detrimental effect on both, hot strength and slag resistance.

Spinel forming castables present a volume increase during use at high temperatures, which has been discussed here in detail. The expansion can be designed by various measures such as content and particle size of the magnesia, cement content or hydratable alumina as alternative binder, particle size and reactivity (specific surface area) of the alumina fines used in the matrix and the amount of silica fume added to the castable. A minimum content of silica fume is mandatory in alumina-magnesia castables to attain the desired castable properties with regards to flow and setting behaviour. It is also required for the formation of some liquid phases at higher temperatures which helps to counterbalance the volume expansion. Even small amounts of silica fume have a clear effect on the hot strength at temperatures above 1300 °C which results in a remarkable difference in HMoR and RuL of in-situ spinel versus preformed spinel castables. However, this behaviour might even be advantageous for some applications.

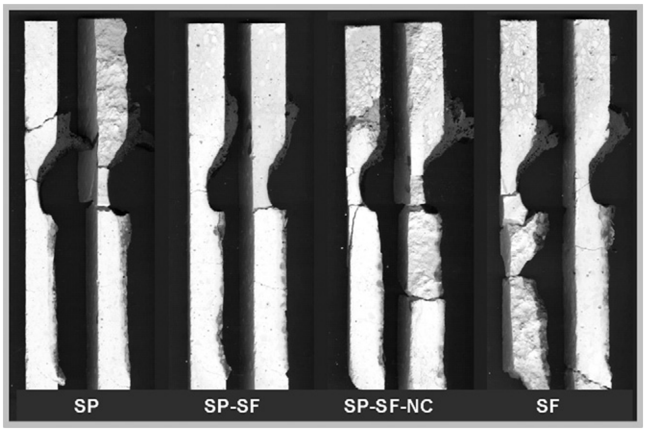

Fig. 39. Test bars of spinel containing and spinel forming castables and mixtures thereof after induction furnace corrosion test 1650°C/2h; CaO:Al_2O_3 ratio 1.08; 6% CaF_2; spinel containing (SP), spinel containing and forming (SP-SF), spinel containing and forming no cement castable (SP-SF-NC) and spinel forming (SF) [103]..

Schnabel et al. [103] have compared the slag resistance of spinel containing and spinel forming castables and mixtures thereof against calcium aluminate steel ladle slag (Fig. 39). Although visually the samples show no major difference, the penetration depth varies in the range of 5.9 - 11.4 mm and is the highest for the alumina-magnesia castable (SF). The cement bonded castables containing pre-reacted spinel show a slightly lower penetration but still higher than the hydratable alumina bonded castable. The wear rates of the castables are very close and in the range of 7 to 8.5 mm/h. The cement bonded castables with *in situ* spinel formation (SF and SP-SF) have the highest corrosion resistance whereas the Alphabond bonded mix (SP-SF-NC) and the spinel containing (SP) corrode at a slightly higher speed.

Fig. 39 - Test bars of spinel containing and spinel forming castables and mixtures thereof after induction furnace corrosion test 1650 °C/2 h; CaO:Al_2O_3 ratio 1.08; 6% CaF_2; spinel containing (SP), spinel containing and forming (SP-SF), spinel containing and forming no cement castable (SP-SF-NC) and spinel forming (SF) [103].

Table 2 summarises the requirements of refractories in different zones of a steel ladle. They can be compared with the properties of preformed and in-situ spinel castables given in Table 3.

In steel ladle bottoms and especially for purging plugs and well blocks, the volumetric stability under high temperature and pressure is most important. High erosion resistance and thermal shock resistance are also important during intensive stirring of the steel and when cold stirring gas is blown through

Table 2
Requirements on refractories in different zones of a steel ladle [103].

	Ladle side wall	Ladle bottom	Impact area (pad)	Purging plug/well block
Thermal stability	++	++	++	+++
Thermo-mechanical stability	+	+++	+++	+++
Erosion resistance	+	++	+++	+++
Corrosion resistance	++	++	+++	++
Potential for stress release	+++	+++	+++	+++

Table 3
Properties of spinel castables by formulation concept [103].

	Spinel	Alumina-magnesia	Alumina-magnesia + spinel	Alumina-magnesia + Spinel/NC
Thermal stability	+++	+	+	++
Thermo-mechanical stability	+++	+	+	++
Erosion resistance	+++	+	+	+
Corrosion resistance	++	++	+++	++
Potential for stress release	+	+++	+++	++

the hot ceramic. Spinel containing castables have become the standard for this application and provide the best performance.

The requirements in steel ladle side walls are different. Each steel ladle shell shows some deformation due to transport, residence, and treatment - the ‘‘water bucket’’ effect. Here it is an advantage if the lining is not absolutely rigid, but shows the ability for stress relaxation to avoid stress peaks which may lead to cracking. The liquid phase formation by the addition of silica fume to spinel forming castables leads to a softening of the castable (steep drop in RuL curve) so that thermal stresses can be released. The volume expansion due to the *in situ* spinel formation can close joints at the surface. Therefore, castables with spinel formation provide advantages in ladle side walls, and the combination of spinel containing and forming might be considered the best solution here.

5. Final remarks and challenges for the future

Although spinel-containing refractory castables present a suitable performance during application in steel ladles and despite the advances attained after evaluating various variables (different binders, magnesia and alumina grain sizes, spinel grains characteristics, proper spinel content, silica fume effect, among others), there is still room for further improvements. Important aspects for spinel forming castables in steel ladle side walls are the expansion of the material under constraint conditions during use and the sintering depth in the lining. Some expansion at the hot side during use is desired because it can close joints and cracks. However, too much expansion can lead to spalling or even damage to the steel shell of the ladle, e.g. the ladle lip ring. Relining techniques are most often required for an economical use of spinel forming castables in steel ladles. Here a balance between higher and lower strength material is required to avoid too many material losses while cleaning the surface, which takes place before relining with fresh castables at the hot side.

Some possibilities for the future would be:

(i) The addition of mineralising and densification compounds: these additives enhance the *in situ* spinel and CA_6 formation at temperatures lower than usual. For the spinel formation, various additives have already been evaluated in the literature, such as boron oxide and other inorganic salts. Nevertheless, the studies published up to now are mainly related to the spinel synthesis instead of spinel-forming castable design. Moreover, other additives known for densifying spinel during sintering, such as titania, were also evaluated, but for pressed samples and again not for refractory castables. Titania presents a well known effect in reducing the firing temperature, keeping a high fired density of alumina materials. However, it also has a detrimental effect on the hot properties which should not be underestimated. Therefore, additional tools for designing the expansion and speeding up the high temperature reactions, should be explored.

(ii) Further evaluation of nano-scaled particles addition: advances in this domain may lead to compositions where the advantages of preformed and *in situ* spinel castables could finally be matched. The reduction of the grain size down to nanometric dimensions could result in high volumetric stability (typical of pre-formed spinels) coupled with better corrosion resistance (characteristic of *in situ* spinels). However, challenges such as avoiding nano particles agglomeration and reducing their costs should be taken into account.

(iii) Thermo-mechanical modelling of *in situ* spinel-forming castables: due to their behaviour and different expansion levels attained when changing the castables' components, the evaluation of the effect of expansion under constraint should be analysed in order to figure out which level of expansion would be suitable to increase the thermo-mechanical performance.

(iv) Post-mortem analyses of the refractory castables applied in the steel ladles: this aspect would result in an iterative feedback effect involving the ladle slags, the steel and the refractory castables, indicating the requirements and routes for the production of advanced spinel-containing refractory castables. Then, to ultimately design castables with the same slag repelling effect as with carbon-bonded graphite containing brick, one would definitively have to add different types of carbon to them. This of course would fundamentally modify the challenges to be overcome and the scope of this review.

Acknowledgments

The authors are grateful to the Federation for International Refractory Research and Education (FIRE) and the Brazilian Research Funding FAPESP for supporting this work.

References

[1] W.D. Kingery, Structure of crystals, in: in: Introduction to Ceramics, John Wiley & Sons, New York, 1960, 81-139.

[2] W.D. Callister, Materials Science and Engineering, 5th ed., John Wiley & Sons, Inc, New York, 2000.

[3] M. Rigaud, R. Landy, Pneumatic steelmaking, Refractories Iron & Steel Society vol. 3 (1996) 68–70.

[4] R.C. Bradt, Mg-Al spinel: is it the mullite of the 21st century? Ref. Appl. and News. 9 (4) (2004) 8–10.

[5] P.R. Racher, R.W. McConnell, A. Buhr, Magnesium aluminate spinel raw materials for high performance refractories for steel ladles, in: *Proceedings of 43rd Conference of Metallurgy*, Hamilton, Canada (2004).

[6] R.E. Moore, B.S. Monton, A. Caballero, Creep behavior of synthetic spinels based on raw diaspore and bauxite, in: *Proceedings of 29th Annual Meeting of St. Louis Section*, St. Louis, USA (1993).

[7] P. Bartha, Spinell und spinellhaltige feuerfeste Werkstoffe, Berichtsband Feuerfesttechnik, Werkstoffe, Rohstoffe, Neue Entwicklungen, Verlag Stahleisen mbH, Düsseldorf, Germany (1984) 113–133.

[8] H. Sumimura, T. Yamamura, Y. Kubota, T. Kaneshige, Study on slag penetration of alumina-spinel castable, in: *Proceedings of UNITECR'99*, Berlin, Germany (1999) 97–101.

[9] K. Fujii, I. Furusato, I. Takita, Composition of spinel clinker for teeming ladle casting materials, Taik. Ov. 12 (1) (1999) 4–9.

[10] G.W. Kriechbaum, C. Wöhrmeyer, G. Routschka, Neue Spinell-Rohstoffe für Feuerfestauskleidungen im Stahlbereich, in: *Proceedings of 35th International Colloquium on Refractories*, Aachen, Germany (1992).

[11] W. Eitel, Monolithic, environment-conscious refractory lining of ladles, in: *Proceedings of 33rd International Colloquium on Refractories*, Aachen, Germany (1990) 420–435.

[12] E Alasaarela, W. Eitel, How infinite is endless lining of ladles?, in: *Proceedings of 34th international colloquium on refractories and UNITECŔ91*, Aachen, Germany (1991).

[13] W. Klan, V. Köster, G. Reuter, H. Wethkamp, Monolithic ladle lining - another contribution to environmentally compatible and cost-conscious steelmaking, in: *Proceedings of 35th international colloquium on refractories*, Aachen, Germany (1992) 103–108.

[14] J. Kärja, H. Nevalaà, Experiences of monolithic ladle linings in Raahe steel works, in: *Proceedings of UNITECR'93*, São Paulo, Brazil (1993) 1312–1319.

[15] J. Mori, Structure change of alumina castable by addition of magnesia or spinel, Taik. Ov. 15 (3) (1995) 20–23.

[16] S. Itose, M. Nakashima, T. Isobe, I. Shimizu, Improvement in the durability of alumina-spinel steel ladle castable containing spinel fine powder, Taik. Ov. 22 (1) (2002) 26–30.

[17] M. Kobayashi, K. Kataoka, Y. Sakamoto, I. Kifune, Use of alumina-magnesia castables in steel ladle sidewalls, Taik. Ov. 17 (3) (1997) 39–44.

[18] A. Nagasoe, S.I. Tsurumoto, A. Kitamura, Refractory characteristics of spinels with various MgO contents, Taik. Ov. 11 (3) (1991) 20–28.

[19] J. Mori, M. Yoshimura, Y. Oguchi, T. Kawakami, I. Ohishi, Effect of slag composition on wear of alumina-spinel castable for steel ladle, Taik. Ov. 12 (1) (1992) 40–45.

[20] B. Naigai, O. Matsumoto, T. Isobe, Y. Nishiumi, Wear mechanism of castasble for steel ladle by slag, Taik. Ov. 12 (1) (1992) 15–20.

[21] Y. Sato, H. Joguchi, N. Hiroki, Test results of alumina-spinel castable for steel ladle, Taik. Ov. 12 (1) (1992) 10–14.

[22] T. Yamamura, Y. Kubota, T. Kaneshige, M. Nanba, Effect of spinel clinker composition on properties of alumina-spinel castable, Taik. Ov. 13 (1994) 39–45.

[23] S. Zhang, W.E. Lee, Spinel-containing refractories, in: Refractories Handbook, C.A. Schacht, Marcel Dekker, Monticello (2004) 81–139.

[24] Y.C. Ko, Properties and production of Al_2O_3-Spinel and Al_2O_3-MgO castables for steel ladles, Ceram. Int. 6 (1) (2002) 51–56.

[25] J. Mori, N. Watanabe, M. Yoshimura, Y. Oguchi, T. Kawakami, A. Matsuo, Material design of monolithic refractories for steel ladle, Am. Ceram. Soc. Bull. 69 (7) (1990) 1172–1176.

[26] P. Reisinger, H. Preßlinger, E. Pissenberger, W. Posch, Evaluation of the interaction of different ladle slags with two different alumina castables, Veitsch-Radex Rundschau 1 (1998) 3–19.

[27] T. Yamamura, Y. Hamazaki, T. Kaneshige, T. Toyoda, M. Nishi, H. Kato, Alumina-spinel castable refractories for steel teeming ladle, Taik. Overs. 12 (1) (1992) 21–27.

[28] A. Buhr, PhD thesis and publication, Tonerdereiche Feuerfestbetone für den Einsatz in der Stahlindustrie (High alumina refractory castables for steel applications), RWTH Aachen, 1996; Stahl und Eisen 116 (9) (1996) 59–66.

[29] G.W. Kriechbaum, V. Gnauck, G. Routschka, The influence of SiO_2 and spinel on the hot properties of high alumina low cement castables, in: *Proceedings of 37th international colloquium on refractories*, Aachen, Germany (1994) 150–159.

[30] Y.C. Ko, Role of spinel composition in the slag resistance of Al_2O_3-spinel and Al_2O_3-MgO castables, Ceram. Int. 28 (2002) 805–810.

[31] A. Molin, J. Molin, J. Podworny, Corrosion mechanism of spinel forming and spinel containing refractory castables in lab and plant conditions, in: *Proceedings of UNITECR'05*, Orlando, USA (2005) 57–62.

[32] S.K. Chen, M.Y. Cheng, S.C. Lin, Y.C. Ko, Thermal characteristics of Al_2O_3-MgO and Al_2O_3-spinel castables for steel ladles, Ceram. Int. 28 (2002) 811–817.

[33] Z. Nakagawa, N. Enomoto, I.S. Yi, K. Asano, Effect of corundum/periclase sizes on expansion behavior during synthesis of spinel, in: *Proceedings of UNITECR'95*, Kyoto, Japan (1995) 1312–1319.

[34] R.E. Carter, Mechanism of solid-state reaction between magnesium oxide and aluminum oxide and between magnesium oxide and ferric oxide, J; Am. Ceram. Soc. 44 (3) (1997) 116–120.

[35] M. Rigaud, S. Palco, N. wang, Spinel formation in the MgO-Al_2O_3 system relevant to basic oxides, in: *Proceedings of UNITECR'95*, Kyoto, Japan (1995) 387–394.

[36] Y. Kiyota, Reduction of permanent linear change of Al_2O_3-MgO castable, in: *Proceedings of UNITECR'07*, Dresden, Germany (2007) 546–549.

[37] R. Dekkers, C.F. Woensdregt, Crystal structural control on surface topology and crystal morphology of normal spinel ($MgAl_2O_4$), J. Cryst. Gr. 236 (2002) 441–454.

[38] K. Fujiyoshi, Synthesis of whisker-like $MgAl_2O_4$ spinel from gibbsite and magnesium acetate, J. Tech. Assoc. Refract. - Japan 22 (4) (2002) 294–301.

[39] S. Hashimoto, A. Yamaguchi, Synthesis of $MgAl_2O_4$ whiskers by an oxidation-reduction reaction, J. Am. Ceram. Soc. 79 (2) (1996) 491–494.

[40] D.D. Jayaseelan, S. Zhang, S. Hashimoto, W.E. Lee, Template formation of magnesium aluminate ($MgAl_2O_4$) spinel microplatelets in molten salt, J. Eur. Ceram. Soc. 27 (2007) 4745–4749.

[41] S. Zhang, D.D. Jayaseelan, G. Bhattacharya, W.E. Lee, Molten salt synthesis of magnesium aluminate spinel powder, J. Am. Ceram. Soc. 89 (2) (2006) 1724–1726.

[42] S. Hashimoto, S. Zhang, W.E. Lee, A. Yamaguchi, Synthesis of magnesium aluminate spinel platelet and magnesium sulfate precursors, J. Am. Ceram. Soc. 86 (11) (2003) 1959–1961.

[43] M.A.L. Braulio, L.R.M. Bittencourt, V.C. Pandolfelli, Magnesia grain size effect on *in situ* spinel refractory castables, J. Eur. Ceram. Soc. 28 (2008) 2845–2852.

[44] M.A.L. Braulio, D.H. Milanez, E.Y. Sako, L.R.M. Bittencourt, V.C. Pandolfelli, Expansion behavior of cement bonded alumina-magnesia refractory castables, Am. Ceram. Soc. Bull. 86 (12) (2007) 9201–9206.

[45] J.E. Kopanda, G. MacZura, Alumina Chemicals Science and Technology Handbook, American Ceramic Society, Westerville, 1990, pp. 171–183.

[46] F. Simonin, Olagnon, S. Maximilien, G. Fantozzi, L.A. Diaz, R. Torrecillas, Thermomechanical behavior of high-alumina refractory castables with synthetic spinel additions, J. Am. Ceram. Soc. 83 (10) (2000) 2481–2490.

[47] J.M. Auvray, C. Gault, M. Huger, Evolution of elastic properties and microstructural changes versus temperature in bonding phases of alumina and alumina-magnesia refractory castables, J. Eur. Ceram. Soc. 27 (2007) 3489–3496.

[48] M.A.L. Braulio, L.R.M. Bittencourt, J. Poirier, V.C. Pandolfelli, Microsilica effects on cement bonded alumina–magnesia refractory castables, J. Techn. Assoc. Refract. - Japan 28 (3) (2008) 180–184.

[49] M. Fuhrer, A. Hey, W.E. Lee, Microstructural evolution in self-forming spinel/calcium aluminate castable refractories, J. Eur. Ceram. Soc. 18 (1998) 813–820.

[50] Y.C. Ko, J.T. Lay, Thermal expansion characteristics of alumina-magnesia and alumina-spinel castables in the temperature range 800̊-1650̊C, J. Am. Ceram. Soc. 83 (11) (2000) 2872–2874.

[51] L. An, H.M. Chan, K.K. Soni, Control of calcium hexaluminate grain morphology in *in-situ* toughened ceramic composites, J. Mat. Sc. 31 (1996) 3223–3229.

[52] C.F. Chan, Y.C. Ko, Effect of CaO content on the hot strength of alumina-spinel castables in the temperature range of 1000̊ to 1500̊C, J. Am. Ceram. Soc. 81 (11) (1998) 2957–2960.

[53] G. Büchel, A. Buhr, D. Gierisch, Bonite - A new raw material alternative for refractory innovations, in: *Proceedings of UNITECR'05*, Orlando, USA (2005) 462–467.

[54] L. Na, H.M. Chan, R-curve behavior of in-situ toughened Al_2O_3:-$CaAl_{12}O_{19}$ Ceramic Composites, J. Am. Ceram. Soc. 79 (12) (1996) 3142–3148.

[55] M. Sato, M. Takata, Y. Koga, S. Iwamoto, Alumina cement for advanced monolithic refractories, Taik. Overs. 19 (3) (1999) 44–48.

[56] M.A.L. Braulio, L.R.M. Bittencourt, V.C. Pandolfelli, Selection of binders for in situ spinel refractory castables, J. Eur. Ceram. Soc. 29 (13) (2009) 2727–2735.

[57] N.M. Khalil, Heat resistance and thermomechanical behaviour of ultra-low and zero cement castables, Brit. Ceram. Trans. 103 (1) (2004) 37–41.

[58] R. Kockegey-Lorenz, G. Büchel, A. Buhr, J.M. Aroni, R.P. Racher, Improved workability of calcia free alumina binder Alphabond for non-cement castables, in: *Proceedings of 47th international colloquium on refractories*, Aachen, Germany (2004) 67–71.

[59] K. Ide, T. Suzuki, K. Asano, T. Nishi, H. Ichikawa, Expansion Behavior of Alumina-Magnesia Castables, J. Techn. Assoc. Refract. - Japan 25 (3) (2005) 202–208.

[60] E.Y. Sako, M.A.L. Braulio, D.H. Milanez, P.O. Brant, V.C. Pandolfelli, Microsilica role in the CA_6 formation in cement-bonded spinel refractory castables, J. Mat. Proc. Techn. 209 (2009) 5552–5557.

[61] E. Y. Sako, M. A. L. Braulio, P. O. Brant, V. C. Pandolfelli, Cement bonded high alumina refractory castables containing pre-formed and in situ spinel, accepted for publication in Ceram. Int.

[62] R.I. Razouk, R.S. Mikhail, The hydration of magnesium oxide from vapor phase, J. Phys. Chem. 62 (1958) 920–925.

[63] A. Kitamura, K. Onizuka, K. Tanaka, Hydration characteristics of magnesia, Taik. Overs. 16 (3) (1995) 3–11.

[64] T. A. Bier, C. Parr, C. Revais, M. Vialle, H. Fryda, Chemical interaction of MgO in spinel forming castables, in: *Proceedings of XXVII Alafar*, Lima, Peru 1998, p. 8.

[65] R. A. Landy, Magnesia refractories, Refractories Handbook, C.A. Schacht, Marcel Dekker, Monticello, 2004, pp. 109-149.

[66] C. Aksel, F. Kasap, A. Sesver, Investigation of parameters affecting grain growth of sintered magnesite refractories, Ceram. Int. 31 (2005) 121–127.

[67] J. Soudier, Understanding and optimisation of MgO hydration resistance and spinel formation mechanisms for increasing performances of DVM used in crucible induction furnaces melting steel, in: *Proceedings of UNITECR'05*, Orlando, USA (2005) 679–683.

[68] M.A.L. Braulio, J.F.R. Castro, C. Pagliosa, L.R.M. Bittencourt, V.C. Pandolfelli, From macro to nanomagnesia: designing the *in situ* spinel expansion, J. Am. Ceram. Soc. 91 (9) (2008) 3090–3093.

[69] S. Bhaduri, S.B. Bhaduri, Microstructural and mechanical properties of nanocrystalline spinel and related composites, Ceram. Int. 28 (2002) 153–158.

[70] M.F.M. Zawrah, A.A. Kheshen, Synthesis and characterization of nano-crystalline $MgAl_2O_4$ ceramic powders by use of molten salts, Br. Ceram. Trans. 101 (2) (2002) 71–74.

[71] M.F. Zawrah, Investigation of lattice constant, sintering and properties of nano Mg-Al spinels, Mat, Sc. and Eng. A 382 (2004) 362–370.

[72] L.B. Kong, J. Ma, H. Huang, $MgAl_2O_4$ spinel phase derived from oxide mixture activated by a high-energy ball milling process, Mat. Lett. 56 (2002) 238–243.

[73] W. Kim, F. Saito, Effect of grinding on synthesis of $MgAl_2O_4$ spinel from a powder mixture of $Mg(OH)_2$ and $Al(OH)_3$, Powder Tech. 113 (2000) 109–113.

[74] K. Changming, N. Yuee, L. Yangzhen, L. Nan, Preparation of $MgAl_2O_4$ nano-powder by mechanical alloying,, in: *Proceedings of UNITECR'07*, Dresden, Germany, 2007, pp. 290-293.

[75] J. Mori, Y. Toritani, S. Tanaka, Development of alumina-magnesia castable for steel ladle, in: *Proceedings of UNITECR'95*, Kiyoto, Japan, 1995, pp. 171-178.

[76] H. Sarpoolaky, K.G. Ahari, W.E. Lee, Influence of *in situ* formation on microstructural evolution and properties of castables refractories, Ceram. Int. 28 (2002) 487–493.

[77] B. Myhre, B. Sandberg, A.M. Hundere, Castables with $MgO-SiO_2-Al_2O_3$ as bond phase, in: *Proceedings of XXVI Alafar*, San Juan, Porto Rico (1997) p10.

[78] F.N. Cunha-Duncan, R.C. Bradt, Synthesis of magnesium aluminate spinels from bauxites and magnesias, J. Am. Ceram. Soc. 85 (12) (2002) 2995–3003.

[79] M. Tawara, K. Fuji, T. Taniguchi, M. Hagiwara, T. kibayashi, M. Tanaka, Application of alumina-magnesia castable in high temperature steel ladles, Taik. Overs. 16 (2) (1996) 17–19.

[80] K. Jono, J. Mori, Y. Toritani, Effect of alumina grain size on spinel formation, Taik. Overs. 16 (3) (1996) 12–16.

[81] H.R. Zargar, F. Golestani Fard, H.R. Rezaie, The influence of nano boehmite on spinel formation in the alumina-magnesia system at low temperatures, J. Ceram. Proc. Research 9 (1) (2008) 46–51.

[82] Z. Zhang, N. Li, Effect of polymorphism of Al_2O_3 on the synthesis of magnesium aluminate spinel, Ceram. Int. 31 (2005) 583–589.

[83] S.H. Risbud, J.A. Pask, $SiO_2-Al_2O_3$ metastable phase equilibrium diagram without mullite, J. Mat. Sc. 13 (1978) 2449–2454.

[84] M.A.L. Braulio, M.F.L. Piva, G.F.L. Silva, V.C. Pandolfelli, *In situ* expansion design by colloidal alumina suspension addition, J. Am. Ceram. Soc. 92 (2) (2009) 559–562.

[85] T. R. Lipinski, C. Tontrup, The use of nano-scaled alumina in alumina-based refractory materials, in: *Proceedings of UNITECR'07*, Dresden, Germany, 2007, pp. 391-393.

[86] R.G. de Sá, W.E. Lee, Nanotechnology for the refractories industry – a foresight perspective, The Refract. Eng., May Issue (2007) 12–19.

[87] K. Lu, Sintering of nanoceramics, Int. Mat. Reviews 53 (1) (2008) 21–38.

[88] B. Myhre, Microsilica in refractory castables - How does microsilica quality influence performance?, in: *Proceedings of UNITECR'05*, Orlando, USA, 2005, 191-195.

[89] I.R. Oliveira, A.R. Studart, R.G. Pileggi, V.C. Pandolfelli, Dispersão e Empacotamento de Partículas - Princípios e Aplicações em Processamento Cerâmico (Dispersion and Particle Packing - Principles and Applications in Ceramic Processing), Fazendo Arte Editiorial São Paulo (2000).

[90] A.H. de Aza, P. Pena, M.A. Rodriguez, R. Torrecillas, S. de Aza, New spinel containing refractory cements, J. Eur. Ceram. Soc. 23 (2003) 737–744.

[91] C. Odegard, B. Myhre, N. Zhou, S. Zhang, Flow and properties of MgO based castables, in: *Proceedings of XXXIII Alafar*, Antigua, Guatemala, 2004, p. 11.

[92] C. Odegard, Z. Chen, B. Myhre, $MgO-SiO_2-H_2O$ bonded MgO based castables, in: *Proceedings of 4th international symposium on refractories*, Dalian, China (2003) p9.

[93] W.E. Lee, W. Vieira, S. Zhang, K.G. Ahari, H. Sarpoolaky, C. Parr, Castable refractory concretes, Int. Mat. Rev. 46 (3) (2001) 145–167.

[94] B. Nagai, O. Matsumoto, T. Isobe, Development of high-alumina castable for steel ladles (findings on spinel formation in alumina-magnesia castable), Taik. Overs. 10 (1) (1990) 23–28.

[95] P. Nandi, A. Grag, B.D. Chattoraj, M.S. Mukhopahyay, Effect of silica and temperature on spinel-based high-alumina castables, Am. Ceram. Soc. Bul. 31 (2000) 65–69.

[96] B.A. Vázquez, A. Caballero, P. Pena, Quaternary system Al_2O_3-CaO-MgO-SiO_2:I, study of the crystallization volume of Al_2O_3, J, Am. Ceram. Soc. 86 (12) (2003) 2195–2199.

[97] B.A. Vázquez, A. Caballero, P. Pena, Quaternary system Al_2O_3-CaO-MgO-SiO_2:II, study of the crystallization volume of $MgAl_2O_4$, J, Am. Ceram. Soc. 88 (7) (2005) 1949–1957.

[98] R.C. Devries, E.F. Osborn, Phase equilibria in high-alumina part of the system CaO-MgO Al_2O_3-SiO_2, J. Am. Ceram. Soc. 40 (1) (1957) 6–15.

[99] M. Nanba, T. Kaneshige, Y. Hamazaki, H. Nishio, I. Ebisawa, Thermal characteristics of castables for teeming ladle, Taik. Overs. 16 (3) (1996) 17–21.

[100] N. Shirama, K. Murakami, I. Shimizu, Development of low sílica wet gunning material for steel ladles, J. Techn. Assoc. Refract. - Japan 22 (2) (2002) 161–163.

[101] M.A.L. Braulio, P.O. Brant, L.R.M. Bittencourt, V.C. Pandolfelli, Microsilica or MgO grain size: Which one mostly affects the in situ spinel refractory castable expansion? Ceram Int. 35 (8) (2009) 3321–3334.

[102] M. Sugawara, K. Asano, The recent developments of castable technology in Japan,? in: *Proceedings of UNITECR'05* Orlando, USA (2005) 30–34.

[103] M. Schnabel, A. Buhr, R. Exenberger, C. Rampitsch, Spinel: in-situ versus preformed - clearing the myth, Refract. W. Forum 2 (2) (2010) 87–93.